

Testing cloud microphysics parameterizations in NCAR CAM5 with ISDAC and M-PACE observations

Xiaohong Liu,¹ Shaocheng Xie,² James Boyle,² Stephen A. Klein,² Xiangjun Shi,^{1,3} Zhien Wang,⁴ Wuyin Lin,⁵ Steven J. Ghan,¹ Michael Earle,⁶ Peter S. K. Liu,⁶ and Alla Zelenyuk¹

Received 1 March 2011; revised 17 October 2011; accepted 26 October 2011; published 24 December 2011.

[1] Arctic clouds simulated by the National Center for Atmospheric Research (NCAR) Community Atmospheric Model version 5 (CAM5) are evaluated with observations from the U.S. Department of Energy (DOE) Atmospheric Radiation Measurement (ARM) Indirect and Semi-Direct Aerosol Campaign (ISDAC) and Mixed-Phase Arctic Cloud Experiment (M-PACE), which were conducted at its North Slope of Alaska site in April 2008 and October 2004, respectively. Model forecasts for the Arctic spring and fall seasons performed under the Cloud-Associated Parameterizations Testbed framework generally reproduce the spatial distributions of cloud fraction for single-layer boundary-layer mixed-phase stratocumulus and multilayer or deep frontal clouds. However, for low-level stratocumulus, the model significantly underestimates the observed cloud liquid water content in both seasons. As a result, CAM5 significantly underestimates the surface downward longwave radiative fluxes by 20–40 W m⁻². Introducing a new ice nucleation parameterization slightly improves the model performance for low-level mixed-phase clouds by increasing cloud liquid water content through the reduction of the conversion rate from cloud liquid to ice by the Wegener-Bergeron-Findeisen process. The CAM5 single-column model testing shows that changing the instantaneous freezing temperature of rain to form snow from –5°C to –40°C causes a large increase in modeled cloud liquid water content through the slowing down of cloud liquid and rain-related processes (e.g., autoconversion of cloud liquid to rain). The underestimation of aerosol concentrations in CAM5 in the Arctic also plays an important role in the low bias of cloud liquid water in the single-layer mixed-phase clouds. In addition, numerical issues related to the coupling of model physics and time stepping in CAM5 are responsible for the model biases and will be explored in future studies.

Citation: Liu, X., et al. (2011), Testing cloud microphysics parameterizations in NCAR CAM5 with ISDAC and M-PACE observations, *J. Geophys. Res.*, 116, D00T11, doi:10.1029/2011JD015889.

1. Introduction

[2] The global averaged temperature on the Earth's surface has increased by 0.7°C over the last two centuries [Intergovernmental Panel on Climate Change, 2007]. In the Arctic, the average temperature has risen almost twice as fast as in the rest of the world. There have been significant efforts in the last decade (e.g., the 1997–1998 Surface Heat

Budget of the Arctic Ocean Experiment, SHEBA [Uttal *et al.*, 2002]; the 2008 International Polar Year) to understand the mechanisms for the Arctic climate change, in which aerosol and clouds are believed to play important roles. For example, black carbon produced from fossil fuel and biomass burning and deposited to the snowpack is an important contributor to the warming of the Arctic through the reduction of snow albedo [e.g., Hansen and Nazarenko, 2004; Flanner *et al.*, 2007; McConnell *et al.*, 2007]. Aerosol can also change cloud microphysical properties in the Arctic through their roles as cloud condensational nuclei (CCN) and ice nuclei (IN) [Lubin and Vogelmann, 2006; Garrett and Zhao, 2006; Blanchet and Girard, 1994]. Polar clouds have substantial impacts on surface radiation budgets, and thus can strongly affect Arctic climate change. The reduction of clouds contributed to the unprecedented 2007 summer sea ice loss by enhancing ice-albedo feedbacks [Kay *et al.*, 2008]. Arctic clouds are often mixed-phase (i.e., liquid and ice coexist), and the interplay between the ice and liquid

¹Pacific Northwest National Laboratory, Richland, Washington, USA.

²Lawrence Livermore National Laboratory, Livermore, California, USA.

³Institute of Atmospheric Physics, Chinese Academy of Science, Beijing, China.

⁴Department of Atmospheric Science, University of Wyoming, Laramie, Wyoming, USA.

⁵Brookhaven National Laboratory, Upton, New York, USA.

⁶Science and Technology Branch, Environment Canada, Downsview, Ontario, Canada.

phase microphysics determines the polar cloud properties [e.g., *Liu et al.*, 2007a; *Xie et al.*, 2008].

[3] Climate models have been used in projections of future climate change, including the Arctic sea ice loss. These models are very sensitive to the representation of mixed-phase cloud processes. Using the Colorado State University climate model, *Fowler and Randall* [1996] showed that the liquid/ice partitioning in mixed-phase clouds can significantly impact cloud optical depth and cloud fraction. However, cloud microphysics in mixed-phase clouds are often crudely represented in climate models. For example, temperature-dependent formulations are often used in the partitioning of total cloud water to liquid and ice in mixed-phase clouds (e.g., *Rasch and Kristjánsson* [1998] in National Center for Atmospheric Research (NCAR) Community Atmospheric Model version 3 (CAM3)) and only single-moment of cloud condensates (i.e., mass mixing ratio of cloud liquid and cloud ice) is predicted. The simplified microphysical parameterizations have limited the ability of climate models to accurately simulate the microphysical and radiative properties of mixed-phase clouds observed during the Atmospheric Radiation Measurement (ARM) Mixed-Phase Arctic Cloud Experiment (M-PACE), which was conducted at its North Slope of Alaska site during October 2004 [*Verlinde et al.*, 2007]. The model errors could be reduced when improved double-moment cloud microphysical schemes are used [*Xie et al.*, 2008; *Klein et al.*, 2009].

[4] Only recently have climate models started to implement double-moment cloud microphysical schemes that prognose both the mass and number mixing ratio of cloud condensates [*Morrison and Gettelman*, 2008, hereinafter as MG08; *Liu et al.*, 2007b; *Ming et al.*, 2007; *Lohmann et al.*, 2007]. Microphysical processes in mixed-phase clouds (e.g., ice nucleation and Wegener-Bergeron-Findeisen (WBF) process) are also explicitly treated in these schemes. For example, the latest version of the NCAR climate model (CAM5) uses the double-moment MG08 scheme and an updated treatment of ice nucleation, vapor deposition on ice crystals and ice supersaturation [*Gettelman et al.*, 2010] to replace the single-moment cloud microphysical scheme that was used in its previous versions (CAM3 and CAM4). One major advantage of two-moment cloud microphysics is that the effective sizes of cloud condensates can be calculated from model predicted mass and number mixing ratios. Thus, cloud radiative and microphysical properties can respond to aerosol changes, that is, the so-called aerosol first and second indirect effects, respectively.

[5] Given the uncertainty in representing various cloud processes in climate models, it is necessary to evaluate these new cloud microphysical schemes using available observations. In this study, we test the new cloud microphysics scheme in CAM5 under both the Cloud-Associated Parameterizations Testbed (CAPT) [*Phillips et al.*, 2004] and the Single-Column Modeling (SCM) test bed [*Randall et al.*, 1996]. To examine the response of Arctic mixed-phase clouds to IN number concentration, we also test a new ice nucleation parameterization developed by *Phillips et al.* [2008] in CAM5. The basic idea of CAPT is to use the short-range weather forecast technique to test different cloud parameterizations used in climate models so that the nature of parameterization errors can be evaluated with field

experiment data before longer-time-scale feedbacks develop. The SCM test bed has been widely used to develop and test physical parameterizations in climate models because of its ability to separate targeted parameterizations from the rest of the large-scale model, and the feasibility to validate model performance directly against available field data. Both CAPT and SCM have been proven as useful ways to understand climate model errors and have become an important component of the climate model development process [*Ghan et al.*, 2000; *Xie et al.*, 2002, 2004, 2008; *Boyle et al.*, 2005, 2008; *Boyle and Klein*, 2010; *Klein et al.*, 2006, 2009; *Wang et al.*, 2009; *Morrison et al.*, 2009].

[6] The data used in this study for model evaluation are mainly obtained from the ARM Indirect and Semi-Direct Aerosol Campaign (ISDAC) conducted in April 2008 near the ARM North Slope of Alaska site. During the field campaign, a cloud radar, a polarized micropulse lidar, an atmospheric emitted radiance interferometer and instruments onboard the National Research Council of Canada Convair-580 aircraft [*McFarquhar et al.*, 2011] were used to collect aerosol, cloud and radiation data relevant to Arctic boundary layer clouds. To further evaluate the model performance in simulating mixed-phase boundary layer (BL) clouds, data obtained from the ARM M-PACE campaign are also used. During M-PACE, persistent single-layer BL mixed-phase clouds were observed on 8–14 October 2004 [*Klein et al.*, 2009].

[7] CAM5 with its finite volume dynamic core at resolution of $1.9^\circ \times 2.5^\circ$ in the horizontal and 30 levels in the vertical is used in this study. For CAPT tests, we initialize CAM5 with the NASA MERRA (Modern Era Retrospective-analysis for Research and Applications) reanalysis data (<http://gmao.gsfc.nasa.gov/research/merra/>) for ISDAC and M-PACE. A series of 36 h forecasts with CAM5 are initialized every day at 0000 UT from the MERRA reanalysis for the entire period of ISDAC and M-PACE, respectively. The data from 12 to 36 h of the forecasts concatenated and averaged into 3 h intervals are used in order to reduce the impact of model spin-up that may occur in the first few hours of an integration. In this forecast range, the atmospheric state is still close to the observation so that model errors can be primarily linked to deficiencies in the model physics. Results at the model grid point that is closest to the ARM Barrow site (156.4W, 71.33N) are compared with the ISDAC and M-PACE observations. We note that on the basis of CAPT tests with the M-PACE case and other ARM cases, the simulated cloud properties are not sensitive to the reanalysis data used.

[8] The SCM tests are used to understand causes for the deficiencies of cloud microphysics revealed in the CAPT tests and to examine sensitivities of modeled mixed-phase clouds to parameterizations of cloud microphysical processes in CAM5. SCM tests are conducted for single-layer BL clouds on 8–9 April of the ISDAC (one of the selected cases for process studies given by *McFarquhar et al.* [2011]). Owing to the lack of sounding data during ISDAC, the required time-varying vertical profiles of the large-scale vertical velocity and horizontal advective tendencies of atmospheric state variables (i.e., the so-called large-scale forcing terms) are obtained from the ECMWF analyses (IFS Cycle 32 r3 T799L91). In general, the ECMWF model captures well the observed cloud systems

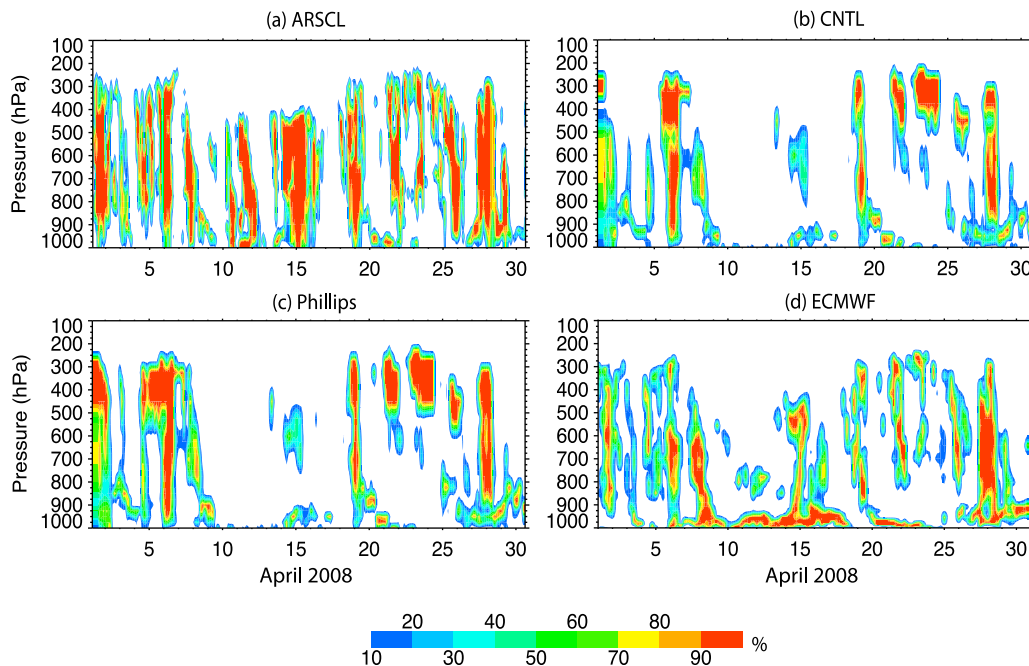


Figure 1. (a) Time-pressure cross section of observed frequency of occurrence of clouds at Barrow from the Active Remotely Sensed Clouds Locations (ARSCL) algorithm. Time-pressure cross section of modeled cloud fraction from (b) the standard CAM5, (c) CAM5 with the *Phillips et al.* [2008] ice nucleation parameterization, and (d) the ECMWF reanalysis during the ISDAC period of April 2008.

on that day (Figure 1), which provides confidence in using the ECMWF forcing to drive the single-column model version of CAM5 (SCAM5). To keep the model’s atmospheric states close to the ECMWF analysis so that we can emphasize the model physics, a nudging approach is used in the SCM tests to nudge the simulated temperature and water vapor toward the analysis at each time step, with a relaxation time scale of 3 h.

[9] This paper is organized as follows: Section 2 provides more details of CAM5 with an emphasis on its cloud microphysical scheme. Section 3 presents the evaluation of modeled clouds and radiation under CAPT with ISDAC and M-PACE observations. Section 4 shows results from SCM tests to examine the sensitivities of CAM5 to parameterizations of cloud microphysical processes. Section 5 concludes this study.

2. Models

2.1. NCAR CAM5

[10] CAM5 was released in June 2010 [Neale *et al.*, 2010]. The physical parameterizations for many model components have been updated. The new modal aerosol module (MAM) (X. Liu *et al.*, Toward a minimal representation of aerosol direct and indirect effects: Model description and evaluation, submitted to *Geoscientific Model Development*, 2011) predicts number as well as mass mixing ratios of multiple aerosol species in three different modes. Aerosol species are internally mixed within a single mode, but externally mixed between modes. With diagnosed subgrid-scale turbulent vertical velocity, MAM activates aerosols with appropriate physical and chemical properties (size distribution and hygroscopicity) for each mode, generating new cloud liquid

droplets and ice crystals through droplet and ice nucleation processes. Thus, CAM5 allows interactive aerosol effects on both warm and cold clouds [Abdul-Razzak and Ghan, 2000; Liu and Penner, 2005]. The cloudy volume in which droplet and ice nucleation occur is more accurately and consistently estimated in the new stratiform cloud macrophysics (S. Park *et al.*, Revised stratiform macrophysics in the Community Atmosphere Model, manuscript in preparation, 2011). Stratiform cloud fraction in CAM5 is obtained from the triangular probability density function (PDF) of total specific humidity using an externally specified half width of the distribution and is a function of the grid mean relative humidity. Aerosol and cloud radiative properties are more accurately taken into account in the new radiation scheme (RRTMG) [Iacono *et al.*, 2008]. The new moist turbulence scheme [Bretherton and Park, 2009] explicitly simulates stratus-radiation-turbulence interactions and makes it possible to simulate thermodynamical and dynamical feedbacks of clouds due to aerosol indirect effects. The new shallow convection scheme [Park and Bretherton, 2009] more accurately simulates the observed spatial distribution of shallow convective activity.

[11] Complex microphysical conversions among cloud liquid droplets, ice crystals, rain and snow are treated by the two-moment stratiform cloud microphysics scheme (MG08) [Gettelman *et al.*, 2008, 2010]. It predicts number concentrations (N_c , N_i) and mass mixing ratios (q_c and q_i) of cloud droplets (subscript c) and cloud ice (subscript i), while the number concentrations and mass mixing ratios of rain and snow (q_r , q_s , N_r , N_s) are diagnosed. The cloud and precipitation particle size distributions are represented by gamma functions. With the predicted N and q for cloud and precipitation particles and specified spectral shape

parameters, the spectral parameters for the size distributions are derived and the effective radii needed for radiation transfer calculations as well as the mass- and number-weighted terminal fall velocities for cloud and precipitation particles are obtained.

[12] MG08 includes the treatment of subgrid cloud variability for cloud liquid water by assuming that the probability density function (PDF) of in-cloud liquid water follows a gamma distribution function. Therefore, enhancement factors of the microphysical process rates for the conversion of cloud liquid to rain by autoconversion and accretion due to subgrid variability of cloud liquid can be derived. Number concentrations and mass mixing ratios of precipitation particles (rain and snow) are determined by neglecting the time tendency term in the conservation equations and numerically integrating downward from the top of the model atmosphere. Two substeps are used to avoid numerical instabilities and to suppress time truncation errors for precipitation processes. The microphysical processes include nucleation of cloud droplets, primary ice nucleation, vapor deposition onto cloud ice, evaporation/sublimation of cloud liquid and ice, conversion of cloud liquid to rain by autoconversion and accretion, conversion of cloud ice to snow by autoconversion and accretion, accretion of cloud liquid by snow, self-collection of snow, self-collection of rain, collection of rain by snow, freezing of cloud liquid and rain, melting of cloud ice and snow, evaporation/sublimation of precipitation, sedimentation of cloud liquid and cloud ice, and convective detrainment of cloud liquid and cloud ice.

[13] The temperature of homogeneous freezing of rain was changed from -40°C in the original MG08 scheme to -5°C in the released version of CAM5 in order to improve the Arctic surface flux and sea ice in the coupled climate simulations [Gettelman *et al.*, 2010]. We note that this change has no physical basis, and thus will not use the term “homogeneous freezing of rain” but use “instantaneous freezing of rain” in the following discussion. The MG08 scheme was further modified for ice microphysics with a process-based treatment of ice supersaturation and ice nucleation [Gettelman *et al.*, 2010]. The supersaturation with respect to ice is allowed for ice and mixed-phase clouds by performing saturation adjustment only for liquid clouds. Water vapor deposition onto ice crystals in mixed-phase and ice clouds is treated with process rate calculations. In mixed-phase clouds, treatment of vapor deposition and the WBF process is similar to MG08. Vapor deposition onto ice occurs if ice is present and is calculated assuming that the in-cloud water vapor mixing ratio is saturated with respect to liquid water.

[14] Ice nucleation is modified by Gettelman *et al.* [2010] to link with aerosol properties on the basis of the work of Liu *et al.* [2007b], which includes homogeneous nucleation of sulfate competing with heterogeneous nucleation on mineral dust [Liu and Penner, 2005] for ice clouds. For mixed-phase clouds, deposition/condensation nucleation is considered on the basis of the work of Meyers *et al.* [1992], with a constant IN number concentration for $T < -20^{\circ}\text{C}$ to be the same as that at $T = -20^{\circ}\text{C}$. The ice supersaturation used by Meyers *et al.* [1992] is calculated from saturated water vapor mixing ratio with respect to liquid in mixed-phase clouds. Contact freezing of cloud droplets by mineral dust and Hallet-Mossop secondary ice production are included and

based on the work of Liu *et al.* [2007b]. Immersion freezing of cloud droplets and rain droplets is based on the work of Bigg [1953] as in MG08.

2.2. CAM5 With a New Ice Nucleation Parameterization

[15] There are still large uncertainties in the mechanisms of ice nucleation, as well as IN properties and number concentrations in the atmosphere. IN number represents only a tiny fraction (less than 0.1%) of aerosol particle populations [DeMott *et al.*, 2010]. Unreliable measurements of ice crystals in clouds due to the shattering of ice crystals on the inlet of probes [Heymsfield, 2007; McFarquhar *et al.*, 2007a] make it difficult to constrain modeled ice crystal properties. The widely used Meyers *et al.* [1992] ice nucleation parameterization was shown to produce too many IN in fall during M-PACE [Prenni *et al.*, 2007]. In addition IN number concentrations in mixed-phase clouds are not predicted but diagnosed from the Meyers *et al.* [1992] parameterization in CAM5. By this implicit sources of IN are assumed that can replenish IN even in regions where they have been scavenged by clouds/precipitation. We note that it is still unclear with IN regeneration mechanisms (e.g., IN formed from drop evaporation residuals as suggested by Fridlind *et al.* [2007]). To quantify the potential impact of lower IN number concentrations on modeled mixed-phase cloud properties, we test another nucleation parameterization from Phillips *et al.* [2008] in CAM5, to replace Meyers *et al.* [1992] parameterization. The Phillips *et al.* [2008] parameterization was developed from the IN measurements by the Colorado State University (CSU) Continuous Flow Diffusion Chamber (CFDC) [Rogers *et al.*, 2001]. Empirical relationships between IN number concentration and surface area densities of aerosol species (mineral dust, black carbon and hydrophobic organics) as well as air temperature were derived. When the parameterization is implemented in CAM5, we use dust and black carbon concentrations provided from the MAM. We neglected the role of hydrophobic organics because of the hydrophilic nature (mixing with other aerosol species) of organics predicted in MAM. We note that IN number concentrations from the Phillips *et al.* [2008] parameterization are much lower (by more than a factor of 10) than those from the parameterization of Meyers *et al.* [1992] in the single-layer mixed-phase clouds during the ISDAC (see section 4.4), consistent with the findings of DeMott *et al.* [2010]. The impact of other ice nucleation parameterizations, for example, the classical-theory-based formulation [Hoose *et al.*, 2010], will be tested in future studies.

3. Results From CAPT Testing

3.1. ISDAC

3.1.1. Modeled Clouds

[16] Several types of clouds were observed at Barrow during the ISDAC period. Figure 1a shows the time-pressure cross section of observed frequency of occurrence of clouds at Barrow. The cloud frequency data obtained from the ARM Climate Modeling Best Estimate (CMBE) product [Xie *et al.*, 2010] are based on integrated measurements from the ARM cloud radars, lidars, and laser ceilometers through the Active Remotely Sensed Clouds Locations (ARSCL)

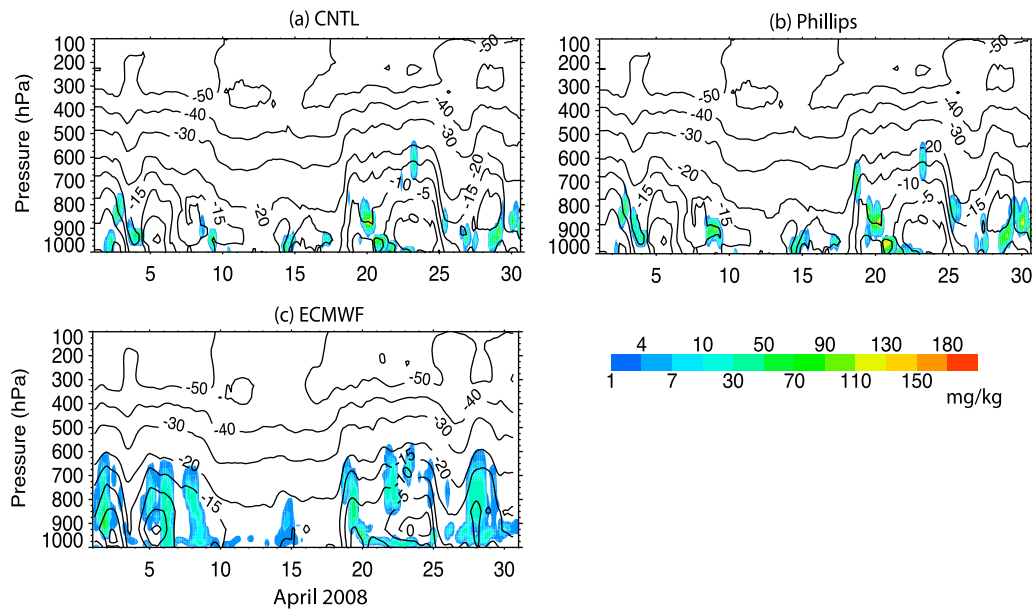


Figure 2. Time-pressure cross section of grid mean liquid water mixing ratio (mg kg^{-1}) from (a) the standard CAM5, (b) CAM5 with the *Phillips et al.* [2008] ice nucleation parameterization, and (c) the ECMWF reanalysis during the ISDAC period of April 2008. Contour lines are for air temperatures in $^{\circ}\text{C}$.

algorithm [*Clothiaux et al.*, 2000]. The data are then averaged from 10 s time and 45 m height intervals to 3 h time and 25 hPa height intervals to better represent clouds over a large-scale global model grid box, which usually represents an area of $200 \text{ km} \times 200 \text{ km}$. As shown in Figure 1a, deep prefrontal and frontal clouds occurred frequently at the Barrow site during the ISDAC, with occasional single-layer BL stratocumulus on 8, 20, 21, and 26 April. As described by *McFarquhar et al.* [2011], the deep frontal clouds during ISDAC were associated with a series of short wave systems propagating around upper level troughs in the Aleutians–Bering Strait area over the North Slope while the low-level stratocumulus clouds formed mostly under high-pressure systems over the Arctic Ocean (we refer the readers to the work of *McFarquhar et al.* [2011] and *Verlinde et al.* [2007] for the map of observation site). Figure 1b shows the cross section of cloud fraction from the CAM5 control run. We note that modeled clouds represent a fraction of a model grid box occupied by clouds, which is different from the radar and lidar detected frequency of occurrence of clouds as shown in Figure 1a. Although averaging the ARSCL cloud data improves the representation of clouds over a global model grid with sizes of 100–200 km, it is still difficult to quantitatively compare cloud fraction simulated by global models with frequency of cloud occurrence obtained from the single point radar and lidar. So the comparison here is to qualitatively evaluate the modeled clouds with the ARM data. Figure 1b shows that CAM5 is able to reproduce the occurrences of many of the deep frontal and single-layer BL clouds observed during the ISDAC. However, large biases exist. CAM5 substantially underestimates the observed deep frontal cloud fraction for the period of 10–18 April. For deep frontal clouds over other periods, CAM5 tends to overestimate clouds at high levels and underestimate them at middle and low levels. In addition, temporal variability of modeled clouds is weaker and lifetime is longer than observed, which

are partially related to the subgrid-scale dynamics that are not resolved in large-scale models [*Xie et al.*, 2008]. This bias may also be due to the fact that the ARSCL observations are from a point location whereas the models are grid box averaged. The simulated clouds are slightly improved in CAM5 with the *Phillips et al.* [2008] ice nucleation parameterization for both the BL stratocumulus in 8–9 April and those deep frontal clouds (Figure 1c). As a reference, we also show in Figure 1d cloud fraction from the ECMWF reanalysis. The observed temporal variability of the deep frontal clouds is better captured by ECMWF than by CAM5, partly owing to the higher resolution (T799L91, which corresponds to a resolution of 0.25°) used in the ECMWF reanalysis compared to $1.9^{\circ} \times 2.5^{\circ}$ L30 used in CAM5. The ECMWF reanalysis shows persistent single-layer BL clouds during 10–18 April that were, however, not evident in the observations. The ECMWF reanalysis also misses the deep frontal clouds observed during 10–12 April.

[17] Figure 2 shows the time-pressure cross section of grid mean cloud liquid water mixing ratio from the standard CAM5, CAM5 with the *Phillips et al.* [2008] ice nucleation parameterization, and from the ECMWF reanalysis during the ISDAC period. We include the ECMWF reanalysis here for the comparison purpose and do not use it for the evaluation of CAM5 since cloud liquid and cloud ice water in the ECMWF reanalysis are not directly assimilated. CAM5 produces considerably less cloud liquid water than ECMWF (Figures 2a and 2c). Cloud liquid mixing ratio is slightly increased with the *Phillips et al.* [2008] ice nucleation parameterization in CAM5 (Figure 2b). It increases by more than 50% for the mixed-phase clouds during some periods (e.g., 8–9 and 20–21 April). This is due to the lower conversion rate of cloud liquid to cloud ice in mixed-phase clouds by the WBF process when the cloud ice number concentrations is reduced with the *Phillips et al.* [2008] parameterization [*Prenni et al.*, 2007; *Liu et al.*, 2007a;

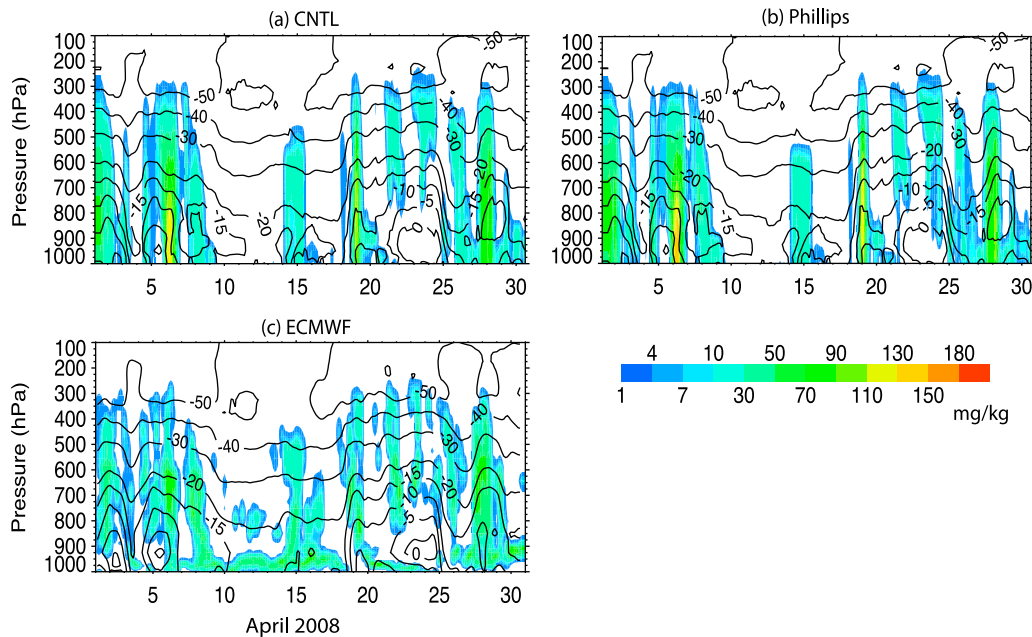


Figure 3. Same as Figure 2 but for total ice water mixing ratio (mg kg^{-1}).

DeMott *et al.*, 2010]. Simulated cloud liquid water content (LWC) for the single-layer BL clouds on 8–9 April is in the range of $0.01\text{--}0.03 \text{ g m}^{-3}$ from the standard CAM5 and $0.01\text{--}0.05 \text{ g m}^{-3}$ from the CAM5 with the Phillips *et al.* [2008] parameterization, both of which are considerably less than in situ aircraft measured LWC of $0.05\text{--}0.4 \text{ g m}^{-3}$ from Flight 16 on 8 April 2008. We note that this comparison of CAM5 results with in situ data is for the reference purpose because of the substantially different temporal and spatial resolution involved in large-scale models (representing a mean of 3 h and $200 \text{ km} \times 200 \text{ km}$ grid size) and in aircraft measurements (10 s and point measurements). LWC was measured from the forward scattering spectrometer probe (FSSP) size particles in the size range of 3 to $47 \mu\text{m}$ [McFarquhar *et al.*, 2011], and the data are available in the ARM data archive.

[18] Figure 3 is the same as Figure 2 except for the total ice water mixing ratio. Since in situ and remote-sensing observations used in this study as well as the ECMWF reanalysis do not differentiate between cloud ice and snow, while CAM5 does, we add CAM5 diagnosed snow amount to cloud ice mixing ratio for better comparison with measurements. In the following, we will use the term “total ice” to represent total mixing ratio of cloud ice and snow. We also note that CAM5 modeled total ice is dominated by snow. As shown in Figure 3, the temporal-spatial distribution of total ice mixing ratio from CAM5 and ECMWF reanalysis closely resembles that of cloud fraction in Figure 1. CAM5 misses the deep frontal clouds during 10–13 April appearing in the ARSCL data. Simulated total ice mixing ratio from the ECMWF reanalysis agrees well with that from CAM5 except that the ECMWF reanalysis shows persistent ice dominated single-layer BL clouds during 16–18 and 21–24 April, which are not present in the ARSCL cloud data. These biases of excessive single-layer BL clouds in the ECMWF reanalysis were also documented by Zhao and Wang [2010]. There are only minor changes in the

total ice mixing ratio with the Phillips *et al.* [2008] parameterization (Figure 3b). Simulated total ice water content (IWC) for the single-layer BL clouds on 8–9 April from both CAM5 simulations is within the range of $0.01\text{--}0.03 \text{ g m}^{-3}$, which is close to the in situ aircraft measured IWC of $0.02\text{--}0.05 \text{ g m}^{-3}$. The measured IWC was derived from composite size distribution measured by the Optical Array Probe two-dimensional cloud probe (2DC) and two-dimensional precipitation probe (2DP) [McFarquhar *et al.*, 2011].

[19] Figure 4 compares the simulated cloud liquid water path (LWP) and ice water path (IWP) from the two CAM5 simulations and from the ECMWF reanalysis with the observations. There are two sources of observed LWP. Both are based on the ARM Climate Facility (ARCF) operational Microwave Radiometer (MWR) measurements, but with different retrieval algorithms. One is based on the algorithm described by Turner *et al.* [2007], and the other one is derived using the work of Wang [2007]. The observed IWP is retrieved from ARM Millimeter Wavelength Cloud Radar (MMCR) and Micropulse Lidar (MPL) measurements using a combined radar-lidar algorithm described by Wang and Sassen [2002]. The mean bias for IWP is expected to be less than 35%. Note that both observed and modeled IWPs include the snow component, because the observations cannot separate snow from ice.

[20] LWPs from the two measurements have similar temporal variations during the ISDAC period, although LWP from Turner *et al.* [2007] is systematically higher by $10\text{--}20 \text{ g m}^{-2}$. Standard CAM5 significantly underestimates the observed LWP, and simulated LWP is less than 10 g m^{-2} during the 5–8, 10–13 and 27–28 April (red line in Figure 4a) when both observations show significant amount ($20\text{--}100 \text{ g m}^{-2}$) of cloud liquid water. CAM5 with the Phillips *et al.* [2008] ice nucleation parameterization agrees better with observations by increasing LWP by more than 50% for some periods (e.g., 8 and 19–20 April) (green line in Figure 4a). However, it overestimates LWP on several

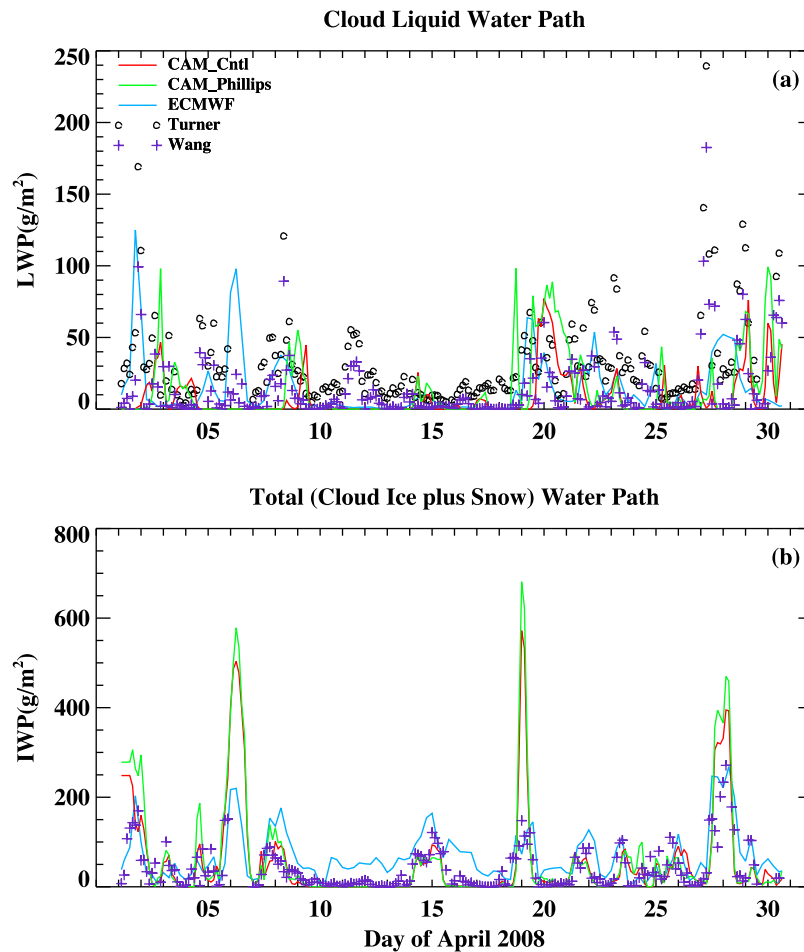


Figure 4. Time series of (a) LWP and (b) IWP. Time series are from the two CAM5 simulations and the ECMWF reanalysis compared with the two LWP measurements (one is from *Turner et al.* [2007] and the other is from *Wang* [2007]) and the IWP measurements from *Wang* [2007] during the ISDAC.

other occasions (e.g., 3 and 18 April). The LWP simulated by ECMWF is also too small for most ISDAC period (blue line in Figure 4a), consistent with *Zhao and Wang's* [2010] results, which showed that ECMWF analysis underestimates LWP for all months statistically. In comparison, CAM5 modeled IWP agrees reasonably well with retrievals (Figure 4b), except on the 6, 19, and 28 April when it overestimates the observations by 30% to a factor of 3. Interestingly, both CAM5 modeled and MMCR/MPL retrieved IWPs are very low (less than 20 g m^{-2}) during the 10–13 April, while ECMWF reanalysis gives an IWP of $40\text{--}80 \text{ g m}^{-2}$ for this period and also for 16–18 April with its persistent BL clouds (Figure 1d). CAM5 with the *Phillips et al.* [2008] ice nucleation parameterization increases the IWP by 10–20% for those deep frontal clouds probably owing to conversion of more cloud liquid to snow in the upper levels, and thus deteriorates the CAM5 simulation.

3.1.2. Modeled Radiation

[21] The modeled cloud fraction, phase and spatial distribution of cloud condensates have a significant impact on modeled radiative fluxes. The ARM Barrow site is located along the coast and has an observed surface albedo of ~ 0.8 during the ISDAC period compared to modeled albedo of ~ 0.7 . The surface albedo has a large impact on surface

shortwave radiation. In general, CAM5 underpredicts the observed downwelling SW flux by up to 100 W m^{-2} for the daytime maximum (figure not shown), which could be partially owing to the smaller surface albedo that leads to a weaker multiple scattering between the surface and cloud layers than the observations. Therefore, we focus on the surface downwelling longwave radiation (LWDN) and the top of atmosphere (TOA) outgoing longwave radiation (OLR) with the observations in this study, since these two fields are related to cloud water content and temperature and not dependent on surface albedo. Figure 5a shows the comparison of modeled and observed downward longwave (LW) radiative fluxes at the surface. The observed surface radiative fluxes are from the ARM Solar and Infrared Radiation Station contained in the CMBE data set [*Xie et al.*, 2010]. There are many fluctuations in the observed surface downward LW fluxes due to the frequent occurrences of deep frontal clouds. Overall, CAM5 reproduces these surface flux variations. However, it tends to underestimate the downward LW fluxes at the surface by $20\text{--}40 \text{ W m}^{-2}$, partly owing to the underestimation of LWP. The underestimation is more severe for 10–18 April, consistent with its missing of large amounts of clouds during this period (Figure 1b). CAM5 with the *Phillips et al.* [2008] ice nucleation

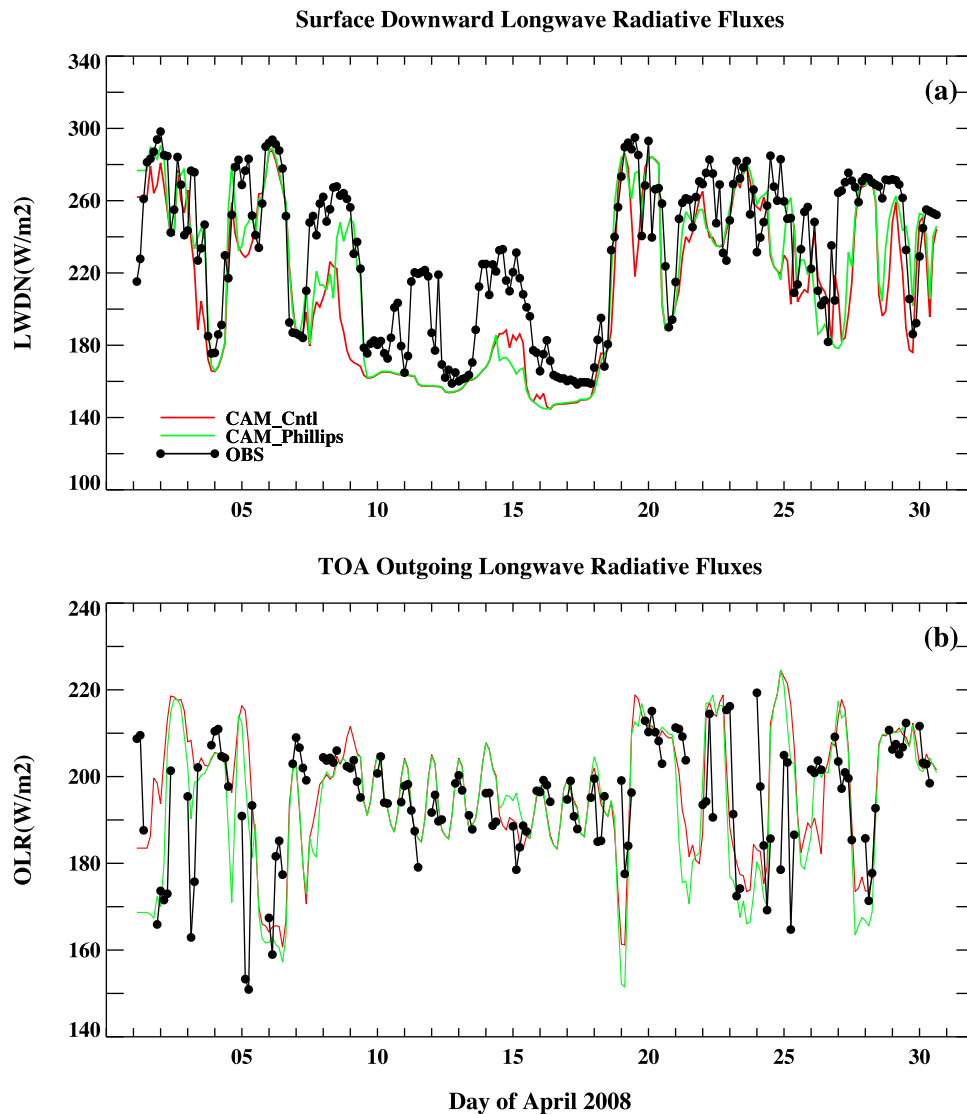


Figure 5. Comparison of modeled and observed (a) downward LW radiative fluxes at surface and (b) outgoing LW radiative fluxes at the top of atmosphere (TOA) during the ISDAC period of April 2008. Observation data are occasionally missing for TOA outgoing LW radiative fluxes.

parameterization slightly improves the simulations, for example, during the 8–9 April, by predicting higher cloud fraction (Figure 1c) and larger LWP (Figure 2b).

[22] Figure 5b shows the TOA OLR fluxes from the model and observations. The observed TOA radiative fluxes are from the $1^\circ \times 1^\circ$ analysis of the NASA CERES measurements (http://eosweb.larc.nasa.gov/PRODOCS/ceres/table_ceres.html). In general, CAM5 reproduces the temporal variations of the TOA OLR fluxes. Consistent with Figure 5a, owing to its lower cloud fraction, it slightly overestimates OLR fluxes, for example, from 10 to 14 April by $\sim 10 \text{ W m}^{-2}$. However, it underestimates the observations during 19–27 April owing to the excessive high-level cloud fraction. There are no significant differences in the modeled OLR fluxes between the standard CAM5 and CAM5 with the *Phillips et al.* [2008] ice nucleation parameterization.

3.2. M-PACE

[23] To further evaluate CAM5 in simulating mixed-phase clouds, CAM5 was run with the NASA MERRA reanalysis for M-PACE. During M-PACE, the ARSCL data indicated that Barrow was covered with persistent single-layer BL stratocumulus with the cloud top around 850 hPa for 8–14 October [*Xie et al.*, 2008]. Our CAPT tests show that CAM5 is able to reproduce the time-pressure distribution of cloud fraction observed during this time period (figure not shown). It underestimates the observed cloud fraction for the period of 12–14 October, which was also shown in the CAPT testing of a development version of CAM5 [*Gettelman et al.*, 2010]. CAM5 with the new ice nucleation parameterization of *Phillips et al.* [2008] slightly improves the simulation for the BL mixed-phase clouds by increasing the cloud fraction. These results are consistent with the findings from the ISDAC tests in section 3.1 (Figure 1).

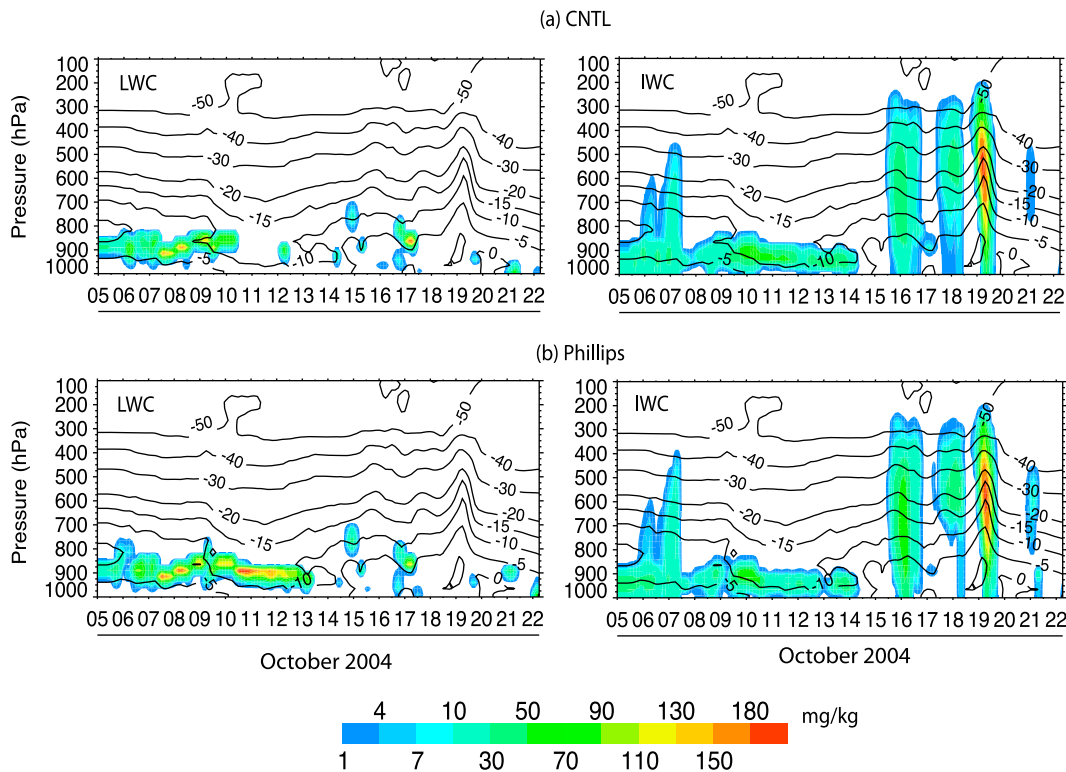


Figure 6. Time-pressure cross section of (left) grid mean liquid water mixing ratio (LWC, mg kg^{-1}) and (right) total ice water mixing ratio (IWC, mg kg^{-1}) from (a) the standard CAM5 and (b) from CAM5 with the ice nucleation parameterization of *Phillips et al.* [2008] during the M-PACE period of October 2004. Contour lines are for air temperatures in $^{\circ}\text{C}$.

[24] Figure 6 shows the grid-box mean cloud liquid and total ice water mixing ratio from the standard CAM5 and CAM5 with the *Phillips et al.* [2008] ice nucleation parameterization for the M-PACE period of October 2004. Liquid water mixing ratio from the standard CAM5 is less than 0.001 g kg^{-1} for the single-layer BL clouds during 10–14 October. Total ice water dominated by snow is better simulated in CAM5. CAM5 with the *Phillips et al.* [2008] ice nucleation parameterization simulates some amount of cloud liquid ($\sim 0.1 \text{ g kg}^{-1}$) for the single-layer BL clouds during 10–13 October. The total ice water mixing ratio for these single-layer clouds is slightly reduced compared to the standard CAM5 simulation owing to the less conversion of cloud liquid to cloud ice through the WBF process. Vertical profiles of cloud fraction and LWC and IWC from model simulations averaged over the period of 9–10 October are compared with the ARSCL measurements [*Clothiaux et al.*, 2000] and remote sensing retrievals [*Shupe et al.*, 2008], as shown in Figure 7. The model simulates the right amount of cloud with appreciable amounts of cloud liquid and with cloud ice and snow precipitating out of the cloud. However, the standard CAM5 simulation underestimates the LWC by 70% and overestimates the IWC by a factor of ~ 2 during this time period. These results in general agree with the findings from *Gettelman et al.* [2010]. The CAM5 simulation with the *Phillips et al.* parameterization increases the LWC by 20% compared to the standard CAM5 with no appreciable change in IWC for this period.

[25] The modeled cloud liquid and total ice water mixing ratio are evaluated from the comparison of observed and

modeled LWP and IWP at Barrow, respectively, as shown in Figure 8. Again, both the observed and modeled IWP include the snow component. The two observations of LWP [*Turner et al.*, 2007; *Wang*, 2007] used here are based on the same retrieval techniques as those for ISDAC, as is the observation of IWP by *Wang and Sassen* [2002]. It can be seen in Figure 8 that the LWP from these two measurements agree with each other very well for the period when the *Wang* [2007] retrievals are available. The observed IWP is available for the single-layer BL mixed-phase clouds from 9 to 15 October. Consistent with results shown in the ISDAC case, CAM5 systematically underestimates the observed LWP for all types of clouds during M-PACE, especially for the single-layer mixed-phase clouds during 8–14 October. CAM5 with the *Phillips et al.* [2008] parameterization improves the modeled LWP for the single-layer mixed-phase clouds from 10 to 13 October by increasing cloud liquid water content (Figure 6). In comparison, CAM5 simulated IWP agrees with observations reasonably well for the single-layer mixed-phase clouds, although it overestimates IWP on 10 October. Compared to the control run, the modeled IWP with the *Phillips et al.* [2008] ice nucleation parameterization is reduced by more than 50% during 11–13 October in these single-layer BL clouds. However, IWP is increased for the deep frontal clouds occurring on 16 and 21 October, which corresponds to an enhanced model bias. This is consistent with the ISDAC tests shown in Figure 4b.

[26] Figure 9 shows the modeled liquid fraction of the total condensate as a function of cloud height compared with

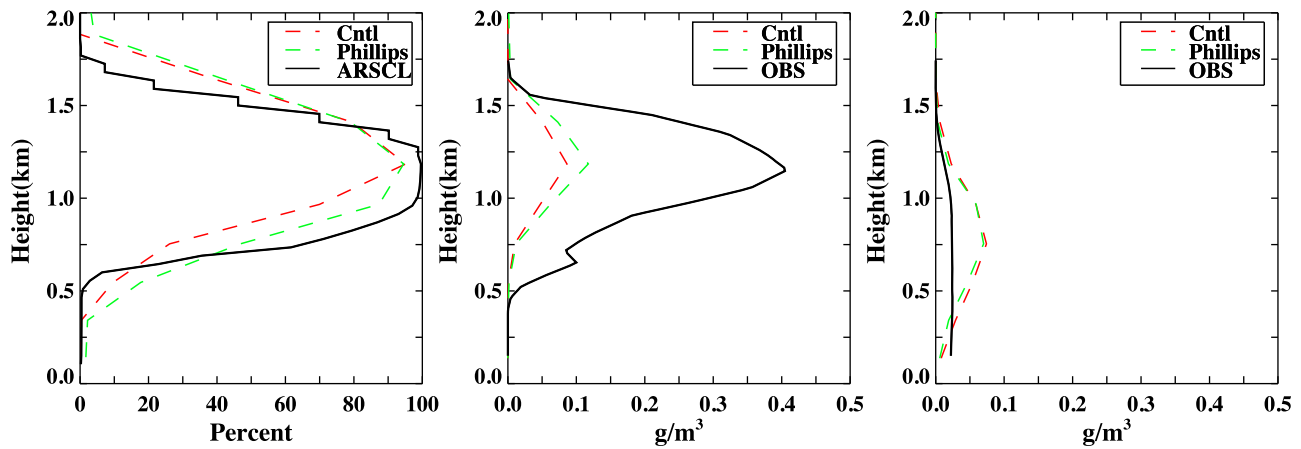


Figure 7. Vertical profiles of (left) cloud fraction (%), (middle) liquid water content, and (right) ice water content, averaged over the period of 1200 UTC, 9 October, to 1200 UTC, 10 October, during M-PACE. Observations are in black. Cloud fraction observations are from ARSCL [Clothiaux *et al.*, 2000]; liquid and ice water content are from Shupe *et al.* [2008]. Simulations for CNTL (red dashed lines) and Phillips *et al.* [2008] parameterization (green dashed lines) are also shown.

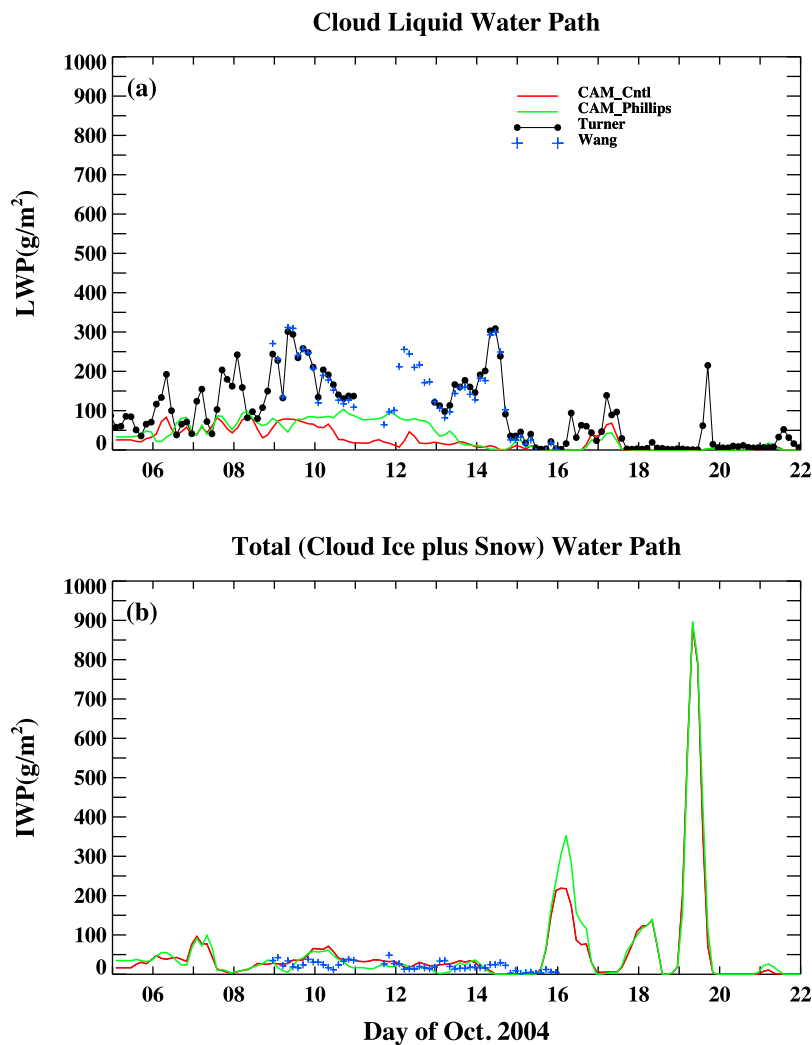


Figure 8. Time series of (a) LWP and (b) IWP, from the two CAM5 simulations compared with retrieved LWP and IWP during the M-PACE period.

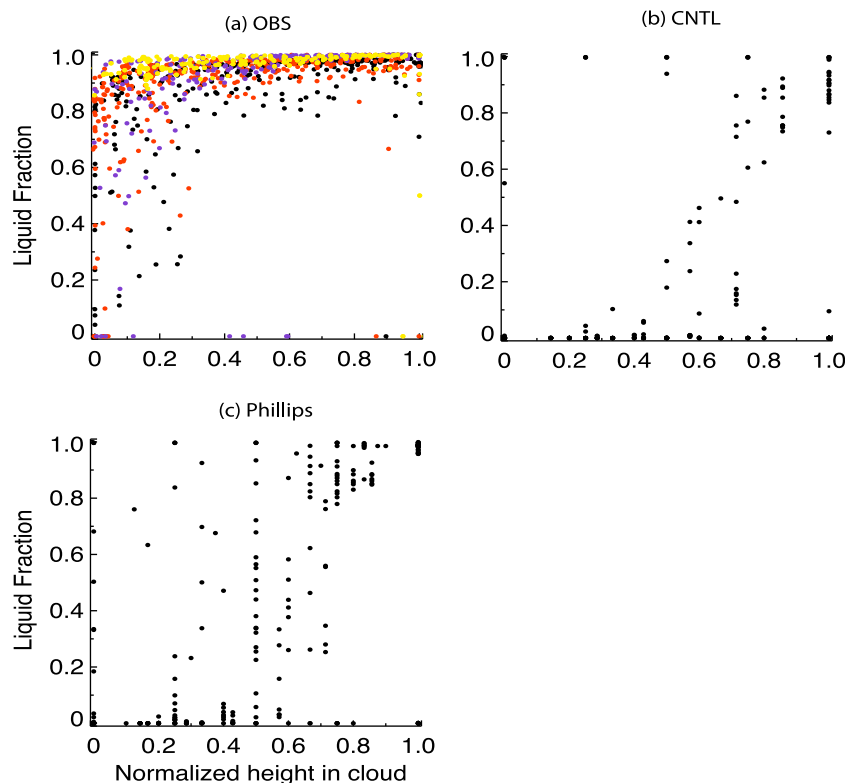


Figure 9. (a) Liquid fraction in the total condensate as a function of cloud height from in situ aircraft observations. The same but from (b) the standard CAM5 and (c) CAM5 with the *Phillips et al.* [2008] ice nucleation parameterization during 9–12 October 2004 of M-PACE period. Colored dots in the observation plot represent four Citation flights (black and red for 9 October, blue for 10 October, and yellow for 12 October).

in situ data obtained on the University of North Dakota Citation aircraft [McFarquhar *et al.*, 2007b] for the single-layer mixed-phase clouds on 9–12 October. This comparison allows us to see if the model can reproduce the statistical features of cloud structure revealed by the aircraft data. In Figure 9, a cloud is defined when the total cloud condensate is larger than 0.001 g m^{-3} for both model results and in situ data [Xie *et al.*, 2008]. The cloud height is normalized from 0 at liquid cloud base to 1 at cloud top. We include the model results for the same period from 9 to 12 October as the aircraft data.

[27] The in situ aircraft data shown in Figure 9a reveal the dominance of cloud liquid water in the BL mixed-phase clouds with temperatures ranging from -12°C to -16°C during this period. In general, the liquid fraction is larger than 0.8 throughout most portions of clouds, with the cloud ice fraction becoming larger in the lower portion of clouds as ice sediments toward cloud base and below. Figures 9b and 9c are for modeled liquid water fraction where snow is added to the total ice for comparison with aircraft data. In general, CAM5 captures the general trend of increasing liquid fraction with cloud height. However, it significantly underestimates the liquid fraction compared with the observations, which is consistent with the underestimation of cloud liquid and approximately correct total ice mixing ratio in Figure 8. CAM5 with the *Phillips et al.* [2008] ice nucleation parameterization slightly improves the agreement of model results with observations, with increased liquid

fraction throughout the clouds (Figure 9c) due to the increased cloud liquid water as shown in Figure 7. However, it still underestimates the liquid fraction compared with observations.

[28] As a result, CAM5 significantly underestimates the downward LW radiative fluxes at the surface by $20\text{--}40 \text{ W m}^{-2}$ from 5 to 12 October and by $80\text{--}100 \text{ W m}^{-2}$ for 13–14 October (figure not shown), owing to its underestimation of cloud liquid mixing ratio. CAM5 with the *Phillips et al.* [2008] parameterization improves the modeled downward LW fluxes for these single-layer BL clouds during 8–12 October by $5\text{--}10 \text{ W m}^{-2}$. CAM5 overestimates the observed OLR from 5 to 15 October by 10 W m^{-2} owing to its underestimation of cloud LWP during this period. There are small differences in modeled OLR between CAM5 and CAM5 with the *Phillips et al.* [2008] ice nucleation parameterization during this period. These results are consistent with the findings from the ISDAC testing (Figure 5).

[29] Compared to CAM3 tested by Xie *et al.* [2008] for M-PACE, CAM5 better simulates the cloud fraction of single-layer BL clouds by simulating higher cloud fractions than CAM3. However, clouds simulated in CAM5 contain significantly less cloud liquid water than those in CAM3. Both CAM5 and CAM3 underestimate the surface downward longwave flux and overestimate the TOA OLR during the period when the single-layer BL clouds occur. Overall, CAM5 performs better with lower radiative flux biases than CAM3. These biases in CAM5 are due to its

Table 1. Aerosol Size Distribution and Mass Fractional Composition Used in the SCAM5 Tests Based on the ISDAC Measurements

	Measured Parameters of Lognormal Distribution ^a	Modes in MAM	Composition in MAM
Mode 1	$N_a = 172.7 \text{ cm}^{-3}$, $D_g = 0.2 \text{ } \mu\text{m}$, $\sigma_g = 1.43$	Accumulation mode	80% (POM), 20% (SO ₄)
Mode 2	$N_a = 5.0 \text{ cm}^{-3}$, $D_g = 1.1 \text{ } \mu\text{m}$, $\sigma_g = 2.35$	Coarse mode	85% (sea salt), 10% (SO ₄), 5% (dust)

^a N_a is total aerosol number; D_g is the mode number mean diameter; and σ_g is the standard deviation of the lognormal distribution.

underestimation in LWP, while those in CAM3 are due to its underestimation in cloud fraction. With a single-moment cloud microphysics scheme and a prescribed partitioning of total water to cloud liquid and ice based on temperature, CAM3 produces opposite trends of height and temperature variation of liquid fraction in total water compared with observations [Liu *et al.*, 2007a]. Another notable difference between CAM5 and CAM3 is that cloud ice is a minor contributor to total ice water content in CAM5, while its amount is higher than that of snow in CAM3 for these single-layer mixed-phase clouds.

4. Sensitivity Tests With SCAM5

[30] In section 3, results from CAPT testing indicate that CAM5 significantly underestimates cloud liquid water content, although the total ice water content (dominated by snow) is relatively well simulated. In order to understand the causes of the underestimation of cloud liquid water content and the dominance of snow in the total ice water, a series of tests were conducted with CAM5 running in single-column mode (SCAM5) to examine the sensitivities of cloud microphysical properties to process parameterizations for the conversions between cloud liquid, cloud ice, rain and snow. The SCAM5 experiments were conducted using the online SCM test bed of the Fast-Physics System Testbed and Research (FASTER) project (<http://www.bnl.gov/esm/>).

[31] The 8–9 April of ISDAC is chosen for our SCAM5 testing. Single-layer boundary layer stratocumulus clouds were observed during this period and there were in situ aircraft measurements of cloud microphysical properties available for model evaluation [McFarquhar *et al.*, 2011]. We ran the SCAM5 for three days starting from 0:00 UTC on 7 April using the nudging approach and results from 19:00 UTC of 8 April to 12:00 UTC of 9 April are used for comparison with observation data. Results for this period are very similar when we started the SCAM5 simulations from 0:00 UTC of 8 April. We found that nudging mainly acts to remove the near-surface warm bias due to the surface driven turbulent mixing during this case. Without nudging, this warm bias would quickly spread throughout the boundary layer and prevent clouds from forming therein. Aerosol fields important for cloud droplet activation and ice nucleation (namely, the aerosol particle size distribution and composition below cloud base) were prescribed from the in situ aircraft measurements. Size distributions were determined from a Particle Measurement Systems (PMS) Passive Cavity Aerosol Spectrometer Probe (PCASP-100X; size range 0.11 – 3 μm with diameter) and PMS Forward Scattering Spectrometer Probe (FSSP-300; size range 0.3 – 20 μm with diameter) following the approach outlined by Earle *et al.* [2011]. Particle size measurements below cloud base on 8–9 April were compiled and averaged to obtain a representative, or “best estimate” distribution for this flight

day. Lognormal fitting parameters for the best estimate aerosol particle size distribution are given in Table 1. The measured accumulation (mode 1) and coarse (mode 2) mode size distributions in Table 1 are assumed to represent the corresponding size modes of MAM in CAM5. Particle composition was measured using a single-particle mass spectrometer, SPLAT II [Zelenyuk *et al.*, 2009]. On the basis of composition analysis from this probe during ISDAC (A. Zelenyuk *et al.*, personal communication, 2011), we prescribed the mass fractional aerosol composition for each MAM mode: 80% organic aerosol and 20% sulfate in the accumulation mode, and 85% sea salt, 10% sulfate and 5% dust in the coarse mode.

[32] The standard SCAM5 simulation shows that cloud fraction is between 0.5 and 1.0 for these single-layer BL clouds. Very little cloud liquid or cloud ice (less than 10^{-6} g m^{-3}) is produced, while the model simulates a significant amount of snow (0.004–0.02 g m^{-3}). The aircraft measured LWC was 0.05–0.4 g m^{-3} , and total IWC was 0.02–0.05 g m^{-3} . To understand the relative importance of cloud microphysical processes in determining the amount of cloud condensates in these single-layer BL clouds, the source and sink terms of cloud liquid, cloud ice, rain and snow averaged between 19:00 UTC of 8 and 12:00 UTC of 9 from the standard SCAM5 are shown in Figure 10. They are calculated from the vertical integration of process rates multiplied by air density divided by liquid water density. We can see from Figure 10 that cloud liquid conversion to snow by the WBF process and autoconversion of cloud liquid to rain are the two most important processes for the loss of cloud liquid in the standard SCAM5 simulation. For rain, production from the autoconversion of cloud liquid is balanced by the loss from the instantaneous freezing of rain and the collection by snow. In comparison, cloud ice-related process rates are very small. In the following, we will conduct a series of SCAM5 sensitivity tests as listed in Table 2 to examine the response of cloud microphysical properties to process parameterizations of cloud microphysics.

4.1. Direct Conversion of Cloud Liquid to Snow

[33] The first test to examine the sensitivity of modeled cloud liquid to cloud microphysical processes is to turn off the direct conversion of cloud liquid to snow. In MG08 there are two direct processes for this conversion: collection of cloud liquid by snow and evaporation of cloud liquid and deposition of water vapor onto snow through the WBF process. By turning off each process separately, or turning both off simultaneously, there were small changes in the simulated cloud liquid mixing ratio. From our budget analysis (figure not shown), when either of the two processes is turned off, autoconversion of cloud liquid to rain speeds up. Therefore, we do not find a strong increase in cloud liquid mixing ratio. We will further test these two processes in section 4.2.

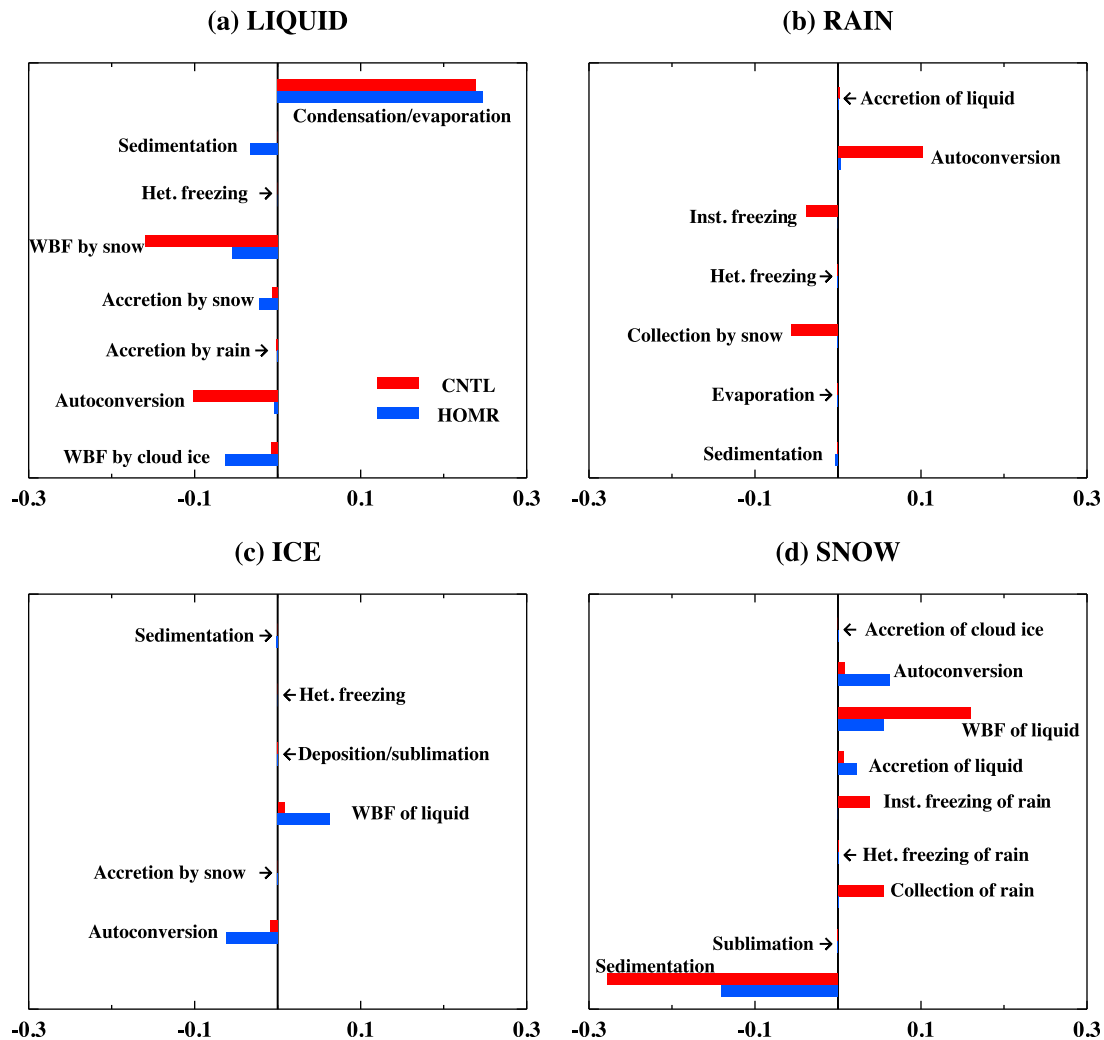


Figure 10. Vertically integrated budgets (mm d^{-1}) of (a) cloud liquid, (b) rain, (c) cloud ice, and (d) snow, from the standard SCAM5 (red bars) and SCAM5 with the instantaneous freezing temperature of rain changed to -40°C (HOMR test, blue bars) averaged between 19:00 UTC of 8 April 2008 and 12:00 UTC of 9 April 2008 during ISDAC. The source and sink terms include large-scale condensation and evaporation of cloud liquid, sedimentation of cloud liquid, heterogeneous freezing of cloud liquid, conversion of liquid to snow by the WBF process, accretion of liquid by snow, accretion of liquid by rain, autoconversion of liquid to rain, conversion of cloud liquid to cloud ice by the WBF process, instantaneous freezing of rain, heterogeneous freezing of rain, collection of rain by snow, evaporation of rain, sedimentation of rain, sedimentation of cloud ice, vapor deposition on cloud ice, accretion of cloud ice by snow, autoconversion of cloud ice to snow, sublimation of snow, and sedimentation of snow. Some term rates (e.g., melting of cloud ice and snow) are negligibly small and thus not shown here.

4.2. Conversion of Rain to Snow: Freezing of Rain

[34] In the model, cloud liquid water can be converted to rain through autoconversion and accretion, and rain can transfer to snow through the freezing of raindrops and the collection of raindrops by snow. There are two mechanisms of rain freezing in MG08: heterogeneous freezing of rain to form snow by immersion freezing [Bigg, 1953] and homogeneous freezing of rain to form snow instantaneously at -40°C . As noted in section 2.1, the temperature of instantaneous freezing of rain is changed to be -5°C in the released version of CAM5 [Gettelman *et al.*, 2010]. Since

temperatures of the Arctic single-layer BL mixed-phase stratocumulus during the ISDAC and M-PACE ranged from -9 to -16°C [McFarquhar *et al.*, 2007b, 2011], rain formed from cloud liquid will instantaneously be converted to snow in these clouds, which will not occur when the instantaneous freezing temperature of rain is set at -40°C . In one test (HOMR) of SCAM5 as listed in Table 2, we reverted the instantaneous freezing temperature of rain to -40°C as in the original MG08. With the shutdown of instantaneous rain freezing in these clouds, rain-related process rates are reduced, while cloud ice-related process rates increased (see blue bars in Figure 10). There is a

Table 2. Summary of SCAM5 Experiments and Simulated Cloud Liquid Water Path (LWP), Total Ice Water Path (IWP), and Cloud Ice Water Path (CIWP) Averaged for the Single-Layer Boundary-Layer Mixed-Phase Clouds From 19:00 UTC of 8 April 2008 to 12:00 UTC of 9 April 2008^a

Name	Experiment Description	LWP (g m ⁻²)	IWP (g m ⁻²)	CIWP (g m ⁻²)
<i>Group a</i>				
CTL	Standard SCAM5	4×10^{-8}	3.36	2×10^{-5}
HOMR	Same as CTL, but homogeneous freezing of rain at -40°C	35.7	1.24	0.043
BERGS	No conversion from cloud liquid to snow by WBF plus HOMR	48.6	0.90	0.048
PSACWS	No accretion of cloud liquid by snow plus HOMR	37.5	1.13	0.050
HETR	No heterogeneous immersion freezing of rain plus HOMR	45.2	1.35	0.043
PRACS	No accretion of rain by snow plus HOMR	36.3	1.23	0.044
<i>Group b</i>				
D CSL	Threshold size of ice to snow of 200 μm plus HOMR	26.8	1.17	0.008
D CSH	Threshold size of ice to snow of 450 μm plus HOMR	28.9	0.82	0.073
INPHIL	<i>Phillips et al.</i> [2008] IN parameterization plus HOMR	53.7	0.17	0.004
Na2	Aerosol number doubled plus HOMR	36.9	1.19	0.043
Na0.2	Aerosol number reduced by five times plus HOMR	18.2	0.73	0.026
<i>Group c</i>				
T	Turner's retrieval for LWP	22.1		
W	Wang's retrieval for LWP and IWP	6.2	22.4	
A	Aircraft measurement	7.1	18.0	

^aRemote sensing retrievals from *Turner et al.* [2007] (denoted as T) and from *Wang* [2007] and *Wang and Sassen* [2002] (denoted as W) and in situ aircraft measurements from *McFarquhar et al.* [2011] (denoted as A) are listed in Group c. LWP and IWP for aircraft measurements are derived by segregating measured LWC and IWC data into 50 m vertical intervals. Mean values of LWP and IWC in each interval are calculated and then integrated vertically to derive the LWP and IWP.

significant decrease in the conversion rate from cloud liquid to snow by the WBF process due to the reduction of snow amount (Table 2), while the conversion rate from cloud liquid to cloud ice by the WBF process is increased. Auto-conversion rate from cloud liquid to rain is significantly reduced owing to the stronger increase in cloud droplet number concentration (CDNC) than that in cloud liquid mixing ratio (autoconversion rate is proportional to cloud liquid mixing ratio and inversely proportional to CDNC). Therefore, cloud microphysical processes are substantially changed in the HOMR test. Modeled cloud fraction increases significantly to 0.9–1.0 for these single-layer BL clouds on 8 and 9 April. There is a substantial amount of cloud liquid ranging from 0.1 to 0.25 g m⁻³, and snow is reduced from 0.004 to 0.02 g m⁻³ in the standard SCAM5 run to 0.001–0.01 g m⁻³. The cloud ice mixing ratio increases to 1×10^{-4} –0.001 g m⁻³, which is still a factor of 4–6 less than that of snow. Cloud droplet and ice crystal number concentrations are in the range of 50–150 cm⁻³, and 1–5 L⁻¹, respectively, both of which are in good agreement with in situ aircraft observations [*McFarquhar et al.*, 2011]. The average LWP, total IWP (cloud ice plus snow), cloud ice water path and snow water path for these single-layer BL clouds are shown in Figure 11. In the following, we will conduct our remaining SCAM5 tests starting from the HOMR scenario; that is, the temperature for instantaneous freezing of rain is set at -40°C . We note that *Gettelman et al.* [2010] performed a CAPT run using the HOMR configuration for the M-PACE case but with a developmental version of CAM5. The HOMR configuration improves the model agreement with the M-PACE observations, consistent with the SCAM result here.

[35] The too fast autoconversion of cloud water to rain-water in the standard CAM5 can be due to the fact that the instantaneous freezing temperature of rain is set at -5°C , as indicated in the HOMR test. In addition, the tendency of

cloud liquid mass due to condensation and tendency of cloud liquid number due to droplet activation are not updated in the same locations in CAM5, which results in unrealistically large droplets and thus high autoconversion rate of cloud liquid to rain, and this efficiently depletes cloud liquid water (P. Caldwell, personal communication, 2011).

[36] In another SCAM5 test, we turned off the heterogeneous immersion freezing of rain (HETR) on top of the HOMR. Cloud liquid water path is increased by $\sim 25\%$ (see Figure 11). There is little change in snow water content for these single-layer mixed-phase stratocumulus clouds because of the compensating effects of a reduction in snow due to less rain freezing and an increase in snow due to more cloud liquid conversion. A test in which the collection of rain by snow (PRACS) was turned off on top of the HOMR shows little effect on modeled cloud liquid and snow (not shown in Figure 11), which suggests that the collection of rain by snow plays a minor role in these single-layer mixed-phase clouds.

[37] We again tested the importance of direct conversion of cloud liquid to snow noted in section 4.1 on top of HOMR (see the two tests BERGS and PSACWS in Table 2). Turning off the WBF process (test BERGS) significantly increases the cloud liquid water content and reduces the snow water content. LWP increases from 35.7 to 48.6 g m⁻² and total IWP is reduced from 1.24 to 0.90 g m⁻² (Table 2). There are smaller effects from PSACWS than from BERGS as shown in Table 2 and Figure 11.

4.3. Conversion of Cloud Ice to Snow: Autoconversion of Cloud Ice

[38] In the CAM5 tests, snow dominates the total ice water content in Arctic single-layer BL mixed-phase stratocumulus clouds. This is also true when the instantaneous freezing temperature of rain to snow is changed from -5°C to -40°C (HOMR). The formulation for the autoconversion of cloud

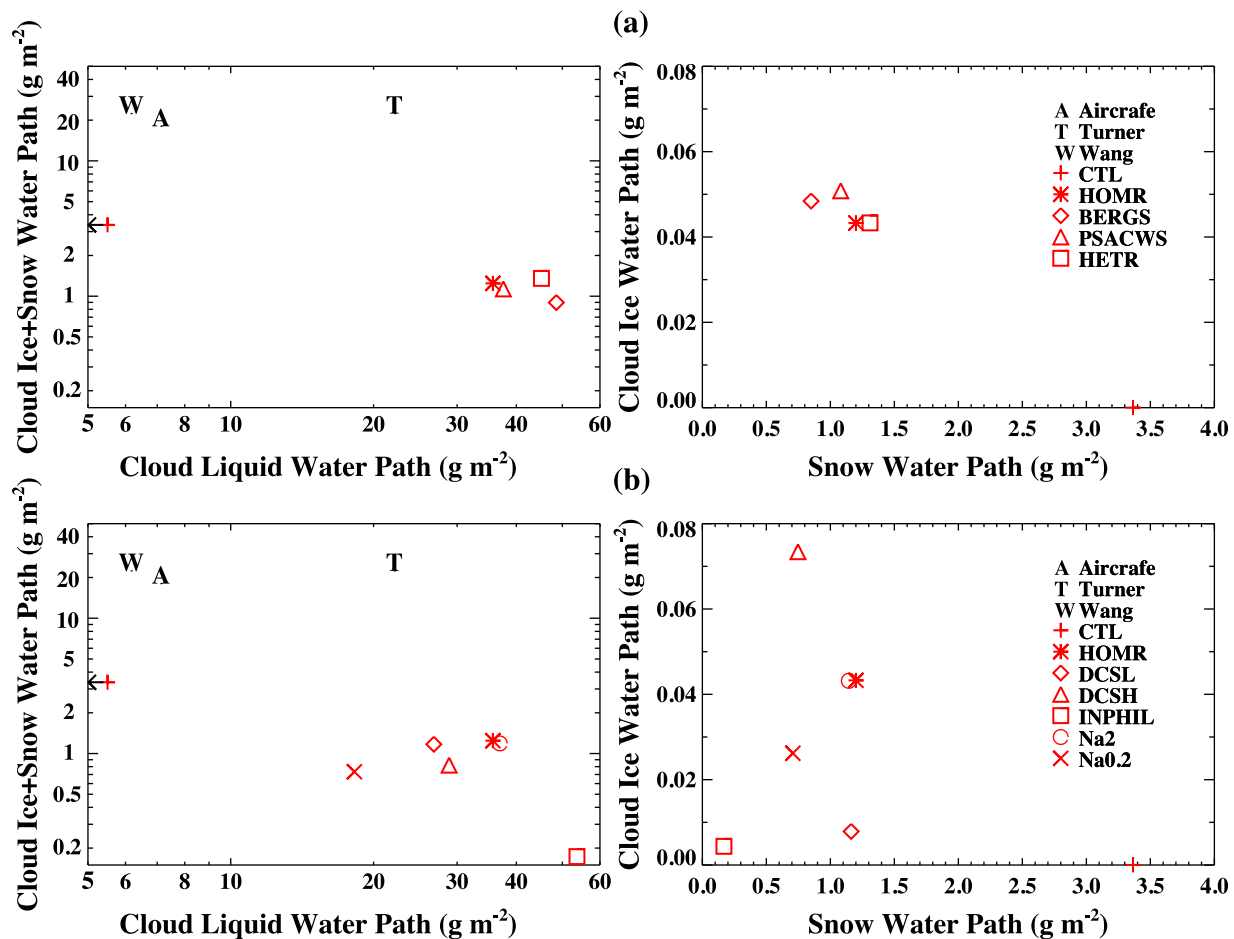


Figure 11. Simulated cloud liquid water path (g m^{-2}), total ice water path (g m^{-2}), snow water path (g m^{-2}), and cloud ice water path (g m^{-2}) averaged for the single-layer boundary-layer mixed-phase clouds from 19:00 UTC of 8 April 2008 to 12:00 UTC of 9 April 2008 during ISDAC for (a) experiment group a and (b) experiment group b (as listed in Table 2). Figure 11 includes measurements from aircraft and remote sensing retrievals as listed in Table 2. The arrows in Figure 11 denote that cloud liquid water from CTL run is out of the range of the x axis.

ice to snow in MG08 is based on the work of *Schoenberg Ferrier* [1994]. There is a threshold size separating cloud ice from snow (D_{cs}), which is largely a tuning parameter. In the original MG08, it was set to $200 \mu\text{m}$, and has been changed to be $325 \mu\text{m}$ in the released version of CAM5. In this subsection, we test different values for D_{cs} between $200 \mu\text{m}$ and $450 \mu\text{m}$. As expected, a decrease of D_{cs} from $325 \mu\text{m}$ to $200 \mu\text{m}$ (test DCSL) results in a faster autoconversion of cloud ice to snow, and reduces the cloud ice water content from $1 \times 10^{-4} - 0.001 \text{ g m}^{-3}$ to less than $1 \times 10^{-5} \text{ g m}^{-3}$. At the same time we see little change in snow water content and a reduction by 25% in cloud liquid water content (Figure 11). Our budget analysis indicates that this reduction of cloud liquid is due to the faster conversion of cloud liquid to snow by the WBF process. An increase in D_{cs} from 325 to $450 \mu\text{m}$ (run DCSH) results in a doubling of cloud ice to $5 \times 10^{-4} - 0.001 \text{ mg m}^{-3}$ and a significant reduction (by 30%) of the snow mixing ratio to $0.001 - 0.002 \text{ g m}^{-3}$. Cloud liquid water content is also reduced by 20% owing to the faster autoconversion of cloud liquid to rain based on the budget analysis, and the total conversion of cloud liquid to cloud ice and snow by the WBF process does

not differ much from the control run (HOMR). The above inconsistency (i.e., a 20% reduction of cloud liquid water, yet the autoconversion rate is higher in DCSH run) is due to the fact that cloud condensate mixing ratios are outputted after the tendencies of cloud microphysical processes are applied, and thus are different from the values used in the tendency calculations. This points out the issue of the long model time step (1200 s). Sensitivity tests with a much smaller time step (20 s) significantly reduce these inconsistencies (P. Caldwell, personal communication, 2011).

4.4. Aerosol Effects on Cloud Microphysical Properties

[39] Aerosol particles can affect cloud microphysical properties by acting as CCN and IN. We tested the sensitivity of CAPT simulated clouds and radiative fluxes to the *Phillips et al.* [2008] ice nucleation parameterization in section 3. In this section we further test this parameterization (test INPHIL in Table 2) on top of the HOMR (i.e., with the instantaneous freezing temperature of rain at -40°C) under the SCAM5 framework. The IN number concentration from test INPHIL is in the range of 0.1 to 0.5 L^{-1} , compared to $1 - 5 \text{ L}^{-1}$ from the parameterization of *Meyers et al.* [1992].

With this order of magnitude reduction in IN number concentration, the conversion rate from cloud liquid to cloud ice by the WBF process is reduced, and thus modeled cloud liquid is enhanced by 50–100%, from 0.1 to 0.25 g m⁻³ to 0.20–0.35 g m⁻³. Both cloud ice and snow mixing ratios are reduced by a factor of 4 for these single-layer BL clouds. The reduction of cloud ice is a result of slower conversion of cloud liquid to ice by the WBF process with lower IN number concentration from the *Phillips et al.* [2008] parameterization, and thus a less efficient production of snow from cloud ice. The sensitivity of simulated cloud properties to the new ice nucleation parameterization is stronger here as compared to the CAPT testing in section 3. This may be due to the speedup of cloud ice-related processes on top of the HOMR in these SCAM5 tests.

[40] CAM5 severely underestimates aerosol optical depth (AOD) by a factor of 5–10 compared with the ARM MultiFilter Rotating Shadowband Radiometer (MFRSR) data during the ISDAC period. Also CAM5 simulated mass concentrations of sulfate and organic aerosol are lower than those estimated from the measured aerosol size distribution and composition for 8–9 April (Table 1) by a factor of 50–100 (figures not shown). These low biases in simulated aerosol in the Arctic were also shown in other studies with CAM5 [*Wang et al.*, 2011; X. Liu et al., Toward a minimal representation of aerosol direct and indirect effects: Model description and evaluation, submitted to *Geoscientific Model Development*, 2011] and with most global models participating in the Aerosol Model Intercomparison Initiative (AeroCom) project [*Koch et al.*, 2009]. Thus we test here the response of cloud microphysical properties to aerosol particle number concentration. With a doubling of prescribed aerosol number concentration in accumulation mode (test Na2 in Table 2), modeled CDNC increases from 50 to 150 cm⁻³ (test HOMR) to 100–300 cm⁻³. We note that in situ aircraft observed CDNC for the single-layer BL clouds in this period is 100–200 cm⁻³ [*McFarquhar et al.*, 2011]. Cloud liquid water content is slightly increased owing to the slower autoconversion of cloud liquid to rain with the increase of CDNC. With a reduction of aerosol number concentration in accumulation mode by a factor of 5 (test Na0.2), CDNC decreases from 50 to 150 to 10–30 cm⁻³. Cloud liquid water content is reduced by a factor of ~2 owing to the faster autoconversion of cloud liquid to rain with the reduction of CDNC. There are ~60% reductions in cloud ice and snow water content. These tests indicate the significant impact of aerosol concentrations on CDNC and cloud water content.

5. Summary and Conclusions

[41] In this study, the MG08 cloud microphysics scheme in CAM5 is evaluated with observations from the ISDAC and M-PACE field campaigns, conducted at the U.S. Department of Energy (DOE) North Slope of Alaska site in April 2008 and October 2004, respectively. We tested the performance of CAM5 in simulating the properties of mixed-phase clouds that occur frequently in the Arctic during spring and autumn. CAM5 was run in the forecast mode under the CAPT framework so that parameterization errors can be evaluated with field data before longer-time-scale feedbacks developed. CAM5 is able to reproduce the

occurrence of several types of clouds (single-layer BL stratocumulus, multilayer and deep frontal clouds) observed during the ISDAC and M-PACE. However, CAM5 misses some deep frontal clouds observed in ISDAC, which is probably caused by the bias in reanalysis data used to initialize CAM5. Also, the temporal variability of frontal clouds is too weak, probably owing to the coarse model resolution and the subgrid-scale dynamics that are not resolved in large-scale models such as CAM5.

[42] CAM5 produces too low cloud liquid water mixing ratio and significantly underestimates the observed LWP for both ISDAC and M-PACE, although it does a much better job in simulating the total ice water content and IWP which are dominated by snow. As a result, observed surface downward longwave radiation flux is underestimated by 20–40 W m⁻² and TOA OLR by 10–20 W m⁻² for both ISDAC and M-PACE, although temporal variations of radiative fluxes are captured reasonably. The two-moment MG08 scheme in CAM5 qualitatively reproduces the increasing trend of the liquid fraction of the total water with altitude for single-layer mixed-phase clouds. However, the liquid fraction is severely underestimated owing to the too low liquid water content. Tests with a new ice nucleation parameterization in CAM5 show slight improvement of modeled cloud liquid water content for the single-layer BL mixed-phase clouds by producing much lower ice crystal number concentrations, and thus slowing down the conversion of cloud liquid to cloud ice through the WBF process.

[43] To understand the causes of the biases in cloud microphysical properties in CAM5 as revealed in the CAPT testing, we performed a series of SCAM5 tests for the single-layer BL clouds observed on 8–9 April during the ISDAC by changing or turning off process parameterizations in MG08. We find that changing the instantaneous freezing temperature of rain from -5°C to -40°C has a substantial impact on the budget of cloud condensates. When rain is not frozen instantaneously to form snow in these single-layer BL clouds, rain-related processes slow down while cloud ice-related processes speed up. Conversion rate from cloud liquid to snow by the WBF process and autoconversion rate of cloud liquid to rain are significantly reduced. In this case when the instantaneous freezing temperature of rain is changed to -40°C, SCAM5 can produce a substantial amount (0.1 to 0.25 g m⁻³) of cloud liquid. When instantaneous freezing of rain does not occur in those BL clouds with temperatures between -9 and -16°C during the ISDAC, accretion of rain by snow plays a negligible role in simulating cloud condensates. Conversions of cloud liquid to cloud ice and to snow through the WBF process are important for cloud liquid, cloud ice and snow mixing ratios, while accretion of cloud liquid by snow is not as important. Our SCAM5 test suggests that the severe underestimation of aerosol concentrations in CAM5 in the Arctic could play an important role in the low bias of cloud liquid water in the single-layer mixed-phase clouds during the ISDAC. In addition, tendencies of cloud liquid water mass and number are not updated in the same locations in CAM5, which results in unrealistically large droplets and thus high autoconversion rate of cloud liquid to rain, and this efficiently depletes cloud liquid water (P. Caldwell, personal communication, 2011). The global impacts of these process parameterizations in CAM5 will be further assessed in a future

study, for example, for the low bias in LWP also revealed in global CAM5 climate runs (Liu et al., submitted manuscript, 2011).

[44] **Acknowledgments.** X. Liu would like to thank H. Morrison for helpful discussion of cloud microphysics in CAM5. Support for X. Liu, X. Shi, and S. J. Ghan was provided by the U.S. Department of Energy (DOE) Office of Science (BER) Atmospheric System Research (ASR) Program and Earth System Modeling Program. Support for J. S. Boyle, S. A. Klein, and S. Xie was provided by the Regional and Global Climate and Earth System Modeling Programs of the Office of Science at the U.S. DOE. Z. Wang acknowledges the support of the DOE under grant DE-FG02-05ER64069. The Pacific Northwest National Laboratory (PNNL) is operated for the DOE by Battelle Memorial Institute under contract DE-AC06-76RLO 1830. The contributions of J. S. Boyle, S. A. Klein, and S. Xie to this work were performed under the auspices of the U.S. Department of Energy by Lawrence Livermore National Laboratory under contract DE-AC52-07NA27344.

References

- Abdul-Razzak, H., and S. J. Ghan (2000), A parameterization of aerosol activation: 2. Multiple aerosol types, *J. Geophys. Res.*, *105*, 6837–6844, doi:10.1029/1999JD901161.
- Bigg, E. K. (1953), The supercooling of water, *Proc. Phys. Soc., Sect. B*, *66*, 688–694.
- Blanchet, J.-P., and E. Girard (1994), Arctic greenhouse cooling, *Nature*, *371*, 383, doi:10.1038/371383a0.
- Boyle, J., and S. A. Klein (2010), Impact of horizontal resolution on climate model forecasts of tropical precipitation and diabatic heating for the TWP-ICE period, *J. Geophys. Res.*, *115*, D23113, doi:10.1029/2010JD014262.
- Boyle, J. S., et al. (2005), Diagnosis of Community Atmospheric Model 2 (CAM2) in numerical weather forecast configuration at Atmospheric Radiation Measurement sites, *J. Geophys. Res.*, *110*, D15S15, doi:10.1029/2004JD005042.
- Boyle, J., S. A. Klein, G. Zhang, S. Xie, R. Pincus, and X. Wei (2008), Climate model forecast experiments for TOGA-COARE, *Mon. Weather Rev.*, *136*, 808–832, doi:10.1175/2007MWR2145.1.
- Bretherton, C. S., and S. Park (2009), A new moist turbulence parameterization in the Community Atmosphere Model, *J. Clim.*, *22*, 3422–3448, doi:10.1175/2008JCLI2556.1.
- Clothiaux, E. E., et al. (2000), Objective determination of cloud heights and radar reflectivities using a combination of active remote sensors at the ARM CART sites, *J. Appl. Meteorol.*, *39*, 645–665, doi:10.1175/1520-0450(2000)039<0645:ODOCHA>2.0.CO;2.
- DeMott, P. J., et al. (2010), Predicting global atmospheric ice nuclei distributions and their impacts on climate, *Proc. Natl. Acad. Sci. U. S. A.*, *107*, 11,217–11,222, doi:10.1073/pnas.0910818107.
- Earle, M. E., P. S. K. Liu, J. W. Strapp, A. Zelenyuk, D. Imre, N. C. Shantz, and W. R. Leitch (2011), Factors influencing the microphysics and radiative properties of liquid-dominated Arctic clouds: Insight from observations of aerosol and clouds during ISDAC, *J. Geophys. Res.*, *116*, D00T09, doi:10.1029/2011JD015887.
- Flanner, M. G., C. S. Zender, J. T. Randerson, and P. J. Rasch (2007), Present-day climate forcing and response from black carbon in snow, *J. Geophys. Res.*, *112*, D11202, doi:10.1029/2006JD008003.
- Fowler, L. D., and D. A. Randall (1996), Liquid and ice cloud microphysics in the CSU general circulation model: 2. Impact on cloudiness, the Earth's radiation budget, and the general circulation of the atmosphere, *J. Clim.*, *9*, 530–560, doi:10.1175/1520-0442(1996)009<0530:LAICMI>2.0.CO;2.
- Fridlind, A. M., A. S. Ackerman, G. McFarquhar, G. Zhang, M. R. Poellot, P. J. DeMott, A. J. Prenni, and A. J. Heymsfield (2007), Ice properties of single-layer stratocumulus during the Mixed-Phase Arctic Cloud Experiment: 2. Model results, *J. Geophys. Res.*, *112*, D24202, doi:10.1029/2007JD008646.
- Garrett, T. J., and C. Zhao (2006), Increased Arctic cloud longwave emissivity associated with pollution from mid-latitudes, *Nature*, *440*, 787–789, doi:10.1038/nature04636.
- Gettelman, A., H. Morrison, and S. J. Ghan (2008), A new two-moment bulk stratiform cloud microphysics scheme in the NCAR Community Atmosphere Model (CAM3), Part II: Single-column and global results, *J. Clim.*, *21*, 3660–3679, doi:10.1175/2008JCLI2116.1.
- Gettelman, A., X. Liu, S. J. Ghan, H. Morrison, S. Park, A. J. Conley, S. A. Klein, J. Boyle, D. L. Mitchell, and J.-L. F. Li (2010), Global simulations of ice nucleation and ice supersaturation with an improved cloud scheme in the Community Atmosphere Model, *J. Geophys. Res.*, *115*, D18216, doi:10.1029/2009JD013797.
- Ghan, S. J., et al. (2000), An intercomparison of single column model simulations of summertime midlatitude continental convection, *J. Geophys. Res.*, *105*, 2091–2124, doi:10.1029/1999JD900971.
- Hansen, J., and L. Nazarenko (2004), Soot climate forcing via snow and ice albedos, *Proc. Natl. Acad. Sci. U. S. A.*, *101*, 423–428, doi:10.1073/pnas.2237157100.
- Heymsfield, A. J. (2007), On measurements of small ice particles in clouds, *Geophys. Res. Lett.*, *34*, L23812, doi:10.1029/2007GL030951.
- Hoose, C., J. E. Kristjansson, J.-P. Chen, and A. Hazra (2010), A classical-theory-based parameterization of heterogeneous ice nucleation by mineral dust, soot, and biological particles in a global climate model, *J. Atmos. Sci.*, *67*, 2483–2503, doi:10.1175/2010JAS3425.1.
- Iacono, M. J., J. S. Delamere, E. J. Mlawer, M. W. Shephard, S. A. Clough, and W. D. Collins (2008), Radiative forcing by long-lived greenhouse gases: Calculations with the AER radiative transfer models, *J. Geophys. Res.*, *113*, D13103, doi:10.1029/2008JD009944.
- Intergovernmental Panel on Climate Change (2007), *Climate Change 2007: The Physical Basis. Contribution of Working Group I to the Fourth Assessment Report of the Intergovernmental Panel on Climate Change*, Cambridge Univ. Press, New York.
- Kay, J. E., T. L'Ecuyer, A. Gettelman, G. Stephens, and C. O'Dell (2008), The contribution of cloud and radiation anomalies to the 2007 Arctic sea ice extent minimum, *Geophys. Res. Lett.*, *35*, L08503, doi:10.1029/2008GL033451.
- Klein, S., X. Jiang, J. Boyle, S. Malyshev, and S. Xie (2006), Diagnosis of the summertime warm and dry bias over the U. S. Southern Great Plains in the GFDL climate model using a weather forecasting approach, *Geophys. Res. Lett.*, *33*, L18805, doi:10.1029/2006GL027567.
- Klein, S. A., et al. (2009), Intercomparison of model simulations of mixed-phase clouds observed during the ARM Mixed-Phase Arctic Cloud Experiment. I: Single-layer cloud, *Q. J. R. Meteorol. Soc.*, *135*, 979–1002, doi:10.1002/qj.416.
- Koch, D., et al. (2009), Evaluation of black carbon estimations in global aerosol models, *Atmos. Chem. Phys.*, *9*, 9001–9026, doi:10.5194/acp-9-9001-2009.
- Liu, X., and J. E. Penner (2005), Ice nucleation parameterization for global models, *Meteorol. Z.*, *14*, 499–514, doi:10.1127/0941-2948/2005/0059.
- Liu, X., S. Xie, and S. J. Ghan (2007a), Evaluation of a new mixed-phase cloud microphysics parameterization with CAM3 single-column model and M-PACE observations, *Geophys. Res. Lett.*, *34*, L23712, doi:10.1029/2007GL031446.
- Liu, X., J. E. Penner, S. J. Ghan, and M. Wang (2007b), Inclusion of ice microphysics in the NCAR Community Atmospheric Model version 3 (CAM3), *J. Clim.*, *20*, 4526–4547, doi:10.1175/JCLI4264.1.
- Lohmann, U., P. Stier, C. Hoose, S. Ferrachat, S. Kloster, E. Roeckner, and J. Zhang (2007), Cloud microphysics and aerosol indirect effects in the global climate model ECHAM5-HAM, *Atmos. Chem. Phys.*, *7*, 3425–3446, doi:10.5194/acp-7-3425-2007.
- Lubin, D., and A. M. Vogelmann (2006), A climatologically significant aerosol longwave indirect effect in the Arctic, *Nature*, *439*, 453–456, doi:10.1038/nature04449.
- McConnell, J. R., R. Edwards, G. L. Kok, M. G. Flanner, C. S. Zender, E. S. Saltzman, J. R. Banta, D. R. Pasteris, M. M. Carter, and J. D. W. Kahl (2007), 20th-Century industrial black carbon emissions altered arctic climate forcing, *Science*, *317*, 1381–1384, doi:10.1126/science.1144856.
- McFarquhar, G. M., J. Um, M. Freer, D. Baumgardner, G. L. Kok, and G. Mace (2007a), Importance of small ice crystals to cirrus properties: Observations from the tropical warm pool international cloud experiment (TWP-ICE), *Geophys. Res. Lett.*, *34*, L13803, doi:10.1029/2007GL029865.
- McFarquhar, G. M., G. Zhang, M. R. Poellot, G. Kok, R. McCoy, T. P. Tooman, A. M. Fridlind, and A. J. Heymsfield (2007b), Ice properties of single layer stratocumulus during the Mixed-Phase Arctic Cloud Experiment: 1. Observations, *J. Geophys. Res.*, *112*, D24201, doi:10.1029/2007JD008633.
- McFarquhar, G. M., et al. (2011), Indirect and Semi-Direct Aerosol Campaign (ISDAC): The impact of Arctic aerosols on clouds, *Bull. Am. Meteorol. Soc.*, *92*, 183–201, doi:10.1175/2010BAMS2935.1.
- Meyers, M. P., P. J. DeMott, and W. R. Cotton (1992), New primary ice nucleation parameterizations in an explicit cloud model, *J. Appl. Meteorol.*, *31*, 708–721, doi:10.1175/1520-0450(1992)031<0708:NPINPI>2.0.CO;2.
- Ming, Y., V. Ramaswamy, L. J. Donner, V. T. J. Phillips, S. A. Klein, P. A. Ginoux, and L. W. Horowitz (2007), Modeling the interactions between aerosols and liquid water clouds with a self-consistent cloud scheme in a general circulation model, *J. Atmos. Sci.*, *64*, 1189–1209, doi:10.1175/JAS3874.1.
- Morrison, H., and A. Gettelman (2008), A new two-moment bulk stratiform cloud microphysics scheme in the Community Atmosphere Model, Version 3 (CAM3). Part I: Description and numerical tests, *J. Clim.*, *21*, 3642–3659, doi:10.1175/2008JCLI2105.1.

- Morrison, H., et al. (2009), Intercomparison of model simulations of mixed-phase clouds observed during the ARM Mixed-Phase Arctic Cloud Experiment. II: Multilayer cloud, *Q. J. R. Meteorol. Soc.*, *135*, 1003–1019, doi:10.1002/qj.415.
- Neale, R. B., et al. (2010), Description of the NCAR Community Atmosphere Model (CAM 5.0), *Tech. Note NCAR/TN-486+STR*, Natl. Cent. for Atmos. Res., Boulder, Colo. June. [Available at http://www.cesm.ucar.edu/models/cesm1.0/cam/docs/description/cam5_desc.pdf.]
- Park, S., and C. S. Bretherton (2009), The University of Washington shallow convection and moist turbulence schemes and their impact on climate simulations with the Community Atmosphere Model, *J. Clim.*, *22*, 3449–3469, doi:10.1175/2008JCLI2557.1.
- Phillips, T. J., et al. (2004), Evaluating parameterizations in GCMs: Climate simulation meets weather prediction, *Bull. Am. Meteorol. Soc.*, *85*, 1903–1915, doi:10.1175/BAMS-85-12-1903.
- Phillips, V. T. J., P. J. DeMott, and C. Andronache (2008), An empirical parameterization of heterogeneous ice nucleation for multiple chemical species of aerosol, *J. Atmos. Sci.*, *65*, 2757–2783, doi:10.1175/2007JAS2546.1.
- Prenni, A. J., J. Y. Harrington, M. Tjernstrom, P. J. DeMott, A. Avramov, C. N. Long, S. M. Kreidenweis, P. Q. Olsson, and J. Verlinde (2007), Can ice nucleating aerosols effect Arctic seasonal climate?, *Bull. Am. Meteorol. Soc.*, *88*, 541–550, doi:10.1175/BAMS-88-4-541.
- Randall, D. A., K.-M. Xu, R. C. J. Somerville, and S. Iacobellis (1996), Single-column models and cloud ensemble models as links between observations and climate models, *J. Clim.*, *9*, 1683–1697.
- Rasch, P. J., and J. E. Kristjánsson (1998), A comparison of the CCM3 model climate using diagnosed and predicted condensate parameterizations, *J. Clim.*, *11*, 1587–1614, doi:10.1175/1520-0442(1998)011<1587:ACOTCM>2.0.CO;2.
- Rogers, D. C., P. J. DeMott, and S. M. Kreidenweis (2001), Airborne measurements of tropospheric ice nucleating aerosol particles in the Arctic Spring, *J. Geophys. Res.*, *106*, 15,053–15,063, doi:10.1029/2000JD900790.
- Schoenberg Ferrier, B. (1994), A double-moment multiple-phase four-class bulk ice scheme, Part I: Description, *J. Atmos. Sci.*, *51*, 249–280, doi:10.1175/1520-0469(1994)051<0249:ADMMPF>2.0.CO;2.
- Shupe, M. D., P. Kollias, P. O. G. Persson, and G. M. McFarquhar (2008), Vertical motions in arctic mixed-phase stratus, *J. Atmos. Sci.*, *65*, 1304–1322.
- Turner, D. D., S. A. Clough, J. C. Liljegren, E. E. Clothiaux, K. Cady-Pereira, and K. L. Gaustad (2007), Retrieving liquid water path and precipitable water vapor from Atmospheric Radiation Measurement (ARM) microwave radiometers, *IEEE Trans. Geosci. Remote Sens.*, *45*, 3680–3690, doi:10.1109/TGRS.2007.903703.
- Uttal, T., et al. (2002), Surface heat budget of the Arctic Ocean, *Bull. Am. Meteorol. Soc.*, *83*, 255–275, doi:10.1175/1520-0477(2002)083<0255:SHBOTA>2.3.CO;2.
- Verlinde, J., et al. (2007), The Mixed-Phase Arctic Cloud Experiment, *Bull. Am. Meteorol. Soc.*, *88*, 205–221, doi:10.1175/BAMS-88-2-205.
- Wang, M., S. J. Ghan, M. Ovchinnikov, X. Liu, R. C. Easter, E. Kassianov, Y. Qian, and H. Morrison (2011), Aerosol indirect effects in a multi-scale aerosol-climate model PNNL-MMF, *Atmos. Chem. Phys. Discuss.*, *11*, 3399–3459, doi:10.5194/acpd-11-3399-2011.
- Wang, W., X. Liu, S. Xie, J. Boyle, and S. A. McFarlane (2009), Testing ice microphysics parameterizations in the NCAR Community Atmospheric Model Version 3 using Tropical Warm Pool–International Cloud Experiment data, *J. Geophys. Res.*, *114*, D14107, doi:10.1029/2008JD011220.
- Wang, Z. (2007), Refined two-channel microwave radiometer liquid water path retrieval at cold regions by using multiple-sensor measurements, *IEEE Geosci. Remote Sens. Lett.*, *4*, 591–595, doi:10.1109/LGRS.2007.900752.
- Wang, Z., and K. Sassen (2002), Cirrus cloud microphysical property retrieval using lidar and radar measurements. Part II: Midlatitude cirrus microphysical and radiative properties, *J. Atmos. Sci.*, *59*, 2291–2302, doi:10.1175/1520-0469(2002)059<2291:CCMPRU>2.0.CO;2.
- Xie, S., et al. (2002), Intercomparison and evaluation of cumulus parameterization under summertime midlatitude continental conditions, *Q. J. R. Meteorol. Soc.*, *128*, 1095–1135, doi:10.1256/003590002320373229.
- Xie, S., M. Zhang, J. S. Boyle, R. T. Cederwall, G. L. Potter, and W. Lin (2004), Impact of a revised convective triggering mechanism on Community Atmosphere Model, Version 2, simulations: Results from short-range weather forecasts, *J. Geophys. Res.*, *109*, D14102, doi:10.1029/2004JD004692.
- Xie, S., J. Boyle, S. A. Klein, X. Liu, and S. Ghan (2008), Simulations of Arctic mixed-phase clouds in forecasts with CAM3 and AM2 for M-PACE, *J. Geophys. Res.*, *113*, D04211, doi:10.1029/2007JD009225.
- Xie, S., et al. (2010), ARM climate modeling best estimate data: A new data product for climate studies, *Bull. Am. Meteorol. Soc.*, *91*, 13–20, doi:10.1175/2009BAMS2891.1.
- Zelenyuk, A., J. Yang, D. Imre, and E. Choi (2009), SPLAT II: An aircraft compatible, ultra-sensitive, high precision instrument for in-situ characterization of the size and composition of fine and ultrafine particles, *Aerosol Sci. Technol.*, *43*, 411–424, doi:10.1080/02786820802709243.
- Zhao, M., and Z. Wang (2010), Comparison of Arctic clouds between European Center for Medium-Range Weather Forecasts simulations and Atmospheric Radiation Measurement Climate Research Facility long-term observations at the North Slope of Alaska Barrow site, *J. Geophys. Res.*, *115*, D23202, doi:10.1029/2010JD014285.

J. Boyle, S. A. Klein, and S. Xie, Lawrence Livermore National Laboratory, Livermore, CA 94550, USA.

M. Earle and P. S. K. Liu, Science and Technology Branch, Environment Canada, 4905 Dufferin St., Downsview, ON M3H 5T4, Canada.

S. J. Ghan, X. Liu, X. Shi, and A. Zelenyuk, Pacific Northwest National Laboratory, WA3200 Q Ave., MSIN K9-24, Richland, WA 99352, USA. (xiaohong.liu@pnnl.gov)

W. Lin, Brookhaven National Laboratory, Upton, NY 11973, USA.

Z. Wang, Department of Atmospheric Science, University of Wyoming, Laramie, WY 82071, USA.